FH University of Applied Sciences TECHNIKUM WIEN

Master thesis

Thesis submitted in partial fulfillment of the requirements for the degree of Master of Science in Engineering at the University of Applied Sciences Technikum Wien - Degree Program Medical Engineering & eHealth

Experimental evaluation of medical nebulizers

By: Bc. Lucia Zajacová
Student Number: 2310228021

Supervisor: FH-Prof. Ing. Richard Pasteka MSc, Ph.D.
Vienna, 18.05. 2024

Author's Declaration

Author:	Bc. Lucia Zajacová
Author's ID:	2310228021
Paper type:	Master's Thesis
Academic year:	2023/2024
Topic:	Experimental evaluation of medical nebulisers

I declare that I have written this paper independently, under the guidance of the advisor and using exclusively the technical references and other sources of information cited in the paper and listed in the comprehensive bibliography at the end of the paper.

As the author, I furthermore declare that, with respect to the creation of this paper, I have not infringed any copyright or violated anyone's personal and/or ownership rights. In this context, I am fully aware of the consequences of breaking Regulation § 11 of the Copyright Act No. 121/2000 Coll. of the Czech Republic, as amended, and of any breach of rights related to intellectual property or introduced within amendments to relevant Acts such as the Intellectual Property Act or the Criminal Code, Act No. 40/2009 Coll. of the Czech Republic, Section 2, Head VI, Part 4.

Vienna 27.5.2024 .....

.....
author's signature*

*The author signs only in the printed version.

ABSTRACT

With the worsening of global atmospheric conditions, the occurrence of respiratory diseases is on the rise, necessitating the development of more efficient devices. Among these devices, medical nebulizers are frequently used for inhalation therapy. While their usability has been repeatedly tested and confirmed, ongoing improvements are desired. This thesis aims to explore existing studies and information to design an experimental setup for evaluating medical nebulizers. The thesis incorporates the utilization of an idealized mechanical upper-airway Alberta model, a breathing simulator xPULM, and an optical aerosol spectrometer PALAS Promo 2000 in combination with the Wellas sensor 2200. Subsequently, it outlines the design of connections between the utilized components and the planning of measurement methods for accurate evaluation. The employed methods provide valuable insights into the characteristics of aerosols produced by the tested nebulizers. Starting from characterization parameters such as nebulizer aerosol output and output rate, residual volume, particle size, and particle size distribution, the evaluation progresses to assessing deposition and establishing the nebulizer efficiency in delivering aerosol particles to different regions of the respiratory tract.

KEYWORDS

medical nebulizer, aerosol particle deposition, aerosol particle characterisation, mechanical upper-airway model, xPULM respiratory system, optical aerosol spectrometery

ABSTRAKT

S narastajúcimi problémami v globálnych atmosférických podmienkach stúpa aj výskyt respiračných ochorení a s ním súvisí aj nárast dopytu po efektívnejších zariadeniach na ich liečbu. Medzi takéto zariadenia patrí aj medicínsky nebulizér, ktorý sa často využíva pri inhalačnej terapii. Aj keď bola jeho účinnosť už mnohokrát overená, stále existuje potreba ďalšieho výskumu a vylepšení. Táto práca sa snaží využiť dostupné štúdie a informácie na vytvorenie experimentálneho prostredia na hodnotenie medicínskych nebulizérov. Obsahuje využitie idealizovaného mechanického modelu horných dýchacích ciest Alberta, dýchacieho simulátora xPULM a optického aerosólového spektrometra PALAS Promo 2000 v kombinácii so senzorom Wellas 2200. Následne sa zameriava na návrh spojení medzi týmito komponentmi a plánovanie metód merania pre presnejšie vyhodnotenie. Tieto metódy poskytujú cenné poznatky o charakteristikách aerosólov produkovaných testovanými nebulizérmi. Výsledkom sú mnohé charakteristické parametre, ako je výstup aerosólu z nebulizéra, jeho rýchlosť, zvyškový objem, veľkosť častíc a ich distribúcia. Hodnotenie sa ďalej sústreďuje na usadenie častíc a stanovenie účinnosti nebulizéra pri dodávaní aerosólových častíc do rôznych častí dýchacieho traktu.

KĽÚČOVÉ SLOVÁ

medicínsky nebulizér, depozícia častíc aerosolí, charakter častíc aerosolí, mechanický model horných dýchacích ciest, xPULM respiračný systém, optická aerosolová spektrometeria

ACKNOWLEDGEMENT

I would like to thank Mr. FH-Prof. Ing. Richard Paštěka, MSc, Ph.D. and Mrs. Lara Alina Schöllbauerfor, MSc for professional guidance, helpfull consultations, patience and support during writing. Next, I would like to thank the entire teaching staff of the Institute of Biomedical Engineering at BUT Brno and teachers from FH Technikum Wien for the acquired knowledge, which greatly contributed to the writing of this thesis.

Contents

Introduction

Respiratory diseases encompass a broad range of conditions affecting the organs responsible for breathing, including the lungs, airways, and respiratory muscles. These conditions can vary widely in their severity and impact, ranging from mild to chronic, life-threatening illnesses. These diseases are a significant global health concern, contributing to substantial morbidity, mortality, and healthcare expenditure, so research into possible and more effective treatment is demanded.

Aerosol science deals with understanding the characteristics of small particles that are suspended in the air, various gases, or even in a vacuum. It focuses on investigating how groups of these particles behave collectively [25]. Aerosol as a form of medication is widely used in the inhalation therapy. Thanks to the direct administration, the required dose is reduced and the pharmaceutical effect is emphasized. Between devices used in this respiration therapy besides pressurized-metered dose inhalers, soft mist inhalers, and dry powder inhalers, nebulizer devices stand as a very user-friendly option often used for pediatric or elderly patients. Propellant-free activation and operation allow accessible treatment with very fine mist with medication wherever and whenever. [20]

After undergoing inhalation therapy, still, just a portion of the prescribed dose reaches its intended destination. Understanding the precise amount of drug deposited is crucial for refining delivery systems or devices to enhance efficiency in targeting specific regions of the respiratory tract.

This thesis focuses on the experimental in vitro evaluation and comparison of different types of nebulizers, that complete the theoretical research and modeling done worldwide on the deposition of aerosol particles in the human respiratory tract. It also focuses on complying with all previously set standards while emphasizing the correction of some revealed shortcomings and limitations for optimizing this pharmacopeial-based testing procedure by reviewing and adjusting an experimental setup and experimental testing methods to achieve high efficiency and accuracy.

Three nebulizers of three types, jet, ultrasonic, and vibrating mesh, were tested in the characterization and particle deposition measurement. The characterization measurement evaluates properties and parameters pre-defined by the manufacturer and compares the nebulizer's performance with each other. In the deposition measurement, the deposition of aerosol particles within the representation of the respiratory tract is analyzed.

1 Anatomy and physiology of the respiratory tract

The main role of the human respiratory system is to ensure the intake of oxygen and the removal of waste carbon dioxide from the body, which enables all living beings to metabolize and function properly. The respiratory system consists of various components such as the central nervous system, the chest wall, the pulmonary circulation, and the respiratory tract. This tract can be categorized into two zones. The nasooropharynx and the conducting airways are placed in the upper part of the tract and are together called the conductive zone. In the lower part of the tract are placed the bronchioles and the alveoli and this part is called the respiratory zone. [1, 2]

1.1 Upper airways

Although the gas exchange of respiration takes place deep within the lungs, it's crucial to recognize the significance of the upper airways, which lie outside the chest. These upper airway structures play a vital role in facilitating and influencing the respiratory process. They serve several functions, including warming, humidifying, and filtering incoming air.

As shown in the figure 1.1, the initial segment of the respiratory tract is the nasopharynx, which begins with the nostrils and the nasal cavity and is divided by the nasal septum into two halves. The nasal passages contain mucous membranes and tiny hair-like structures called cilia, which trap foreign particles. The nasal cavity itself consists of the superior, middle, and inferior turbinates. The roof and posterior wall contain the adenoids, a mass of lymphoid tissue that helps in immune defense. The openings of the Eustachian tubes are present in the lateral walls and equalize the pressure to maintain optimal conditions for hearing and on the superior wall of the nasopharynx, pharyngeal tonsils are located, contributing to the body's immune response. [2, 3]

The oropharynx is the middle part of the pharynx that starts just behind the soft palate, a muscular structure at the back of the roof of the mouth. It contains a set of palatine and lingual tonsils made of lymphatic tissue. A part of the oropharynx is also the base of the tongue and epiglottis, which take place in proper swallowing and articulation. [2, 3]

The nasopharynx joins the oropharynx to the lowest part of the pharynx -the laryngopharynx. It is situated behind the larynx and extends downward to the

esophagus [2, 3]. Epiglottis and laryngeal muscles ensure the proper passage of food and air, ensuring that food enters the esophagus while air travels into the trachea.

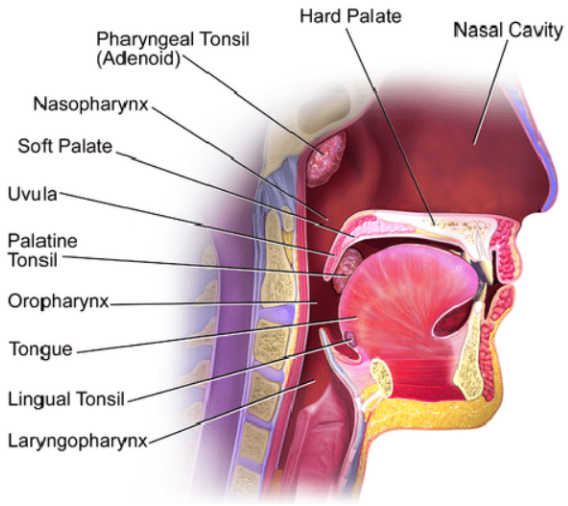

Fig. 1.1: Upper airways structure [4].

1.2 Lower airways

1.2.1 Trachea

The following section described in the figure 1.2 involves the conductive and respiratory air pathways. They initiate with the trachea and are divided into around 23 generations of branchings. The trachea (generation 0) originates from the larynx and at the carina splits into the right and left mainstem bronchi leading to terminal bronchioles (generation 23) [2]. Structurally, the trachea comprises 16 to 20 C-shaped cartilage rings that are stacked on top of each other and are connected by delicate membranes. Behind the trachea lies the anterior portion of the esophagus. [5]

1.2.2 Tracheobronchial tree

Primary bronchi

The left and right main bronchi form the tracheobronchial tree of the lungs. The tracheas' function is to transport air from the oral and nasal passages to the lungs. Subsequently, the bronchi distribute the air throughout the pulmonary structures, facilitating the dispersion of air into the respiratory bronchioles and alveolar sacs within the lungs. The primary bronchi enter the lungs through the hila asymmetrically. The right main bronchus is shorter, wider, and positioned more vertically

compared to the hilum. On the other hand, the left main bronchus is narrower, horizontally oriented, and requires passage below the aortic arch, anterior to the esophagus, and alongside the thoracic aorta to access the hilum of the left lung. [6]

Secondary lobar bronchi

Each primary bronchi subdivide into the secondary lobar bronchi for each lobe of the lungs. The right lung is composed of the upper, middle, and lower lobes, which means it contains 3 secondary lobar bronchi. The left main bronchus divides into two secondary lobar bronchi leading to two lobes of the left lung. [6]

Tertiary segmental bronchi

Afterward, every lobar bronchus branches out into multiple tertiary segmental bronchi. These segmental bronchi individually provide air to a bronchopulmonary segment, which stands as the most substantial division within a lobe. The right lung consists of ten bronchopulmonary segments, while the left lung comprises eight to ten bronchopulmonary segments. [6]

Following the tertiary segmental bronchi, further division leads to bronchioles, which can be categorized into three types: conducting, terminal, and respiratory. As the bronchioles become smaller in diameter, they transition into terminal bronchioles, which signify the conclusion of the conducting zone within the respiratory system. [6]

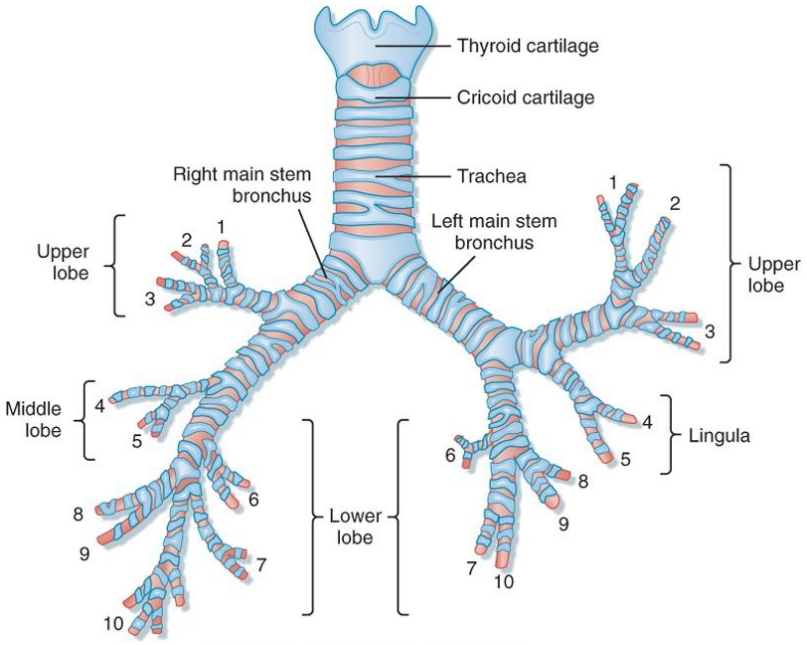

Fig. 1.2: Tracheobronchial tree structure [8].

Terminal respiratory bronchi

Terminal bronchioles eventually bifurcate into multiple generations visible in the figure 1.3 of respiratory bronchioles, which represent the narrowest air passages in the lungs. These bronchioles act as the final pathway leading to the alveoli forming the respiratory zone. They serve as a potential area for trapping smaller foreign particles and also host lymphatic channels. The single-layered epithelial cells forming the lining of the respiratory tract transition into the cells that make up the inner surface of the alveoli. Each respiratory bronchiole branches into two to eleven alveolar ducts, with each duct giving rise to five to six alveolar sacs. [1, 6]

Alveolar region

Recent findings showed that the shape and structure of alveoli is more complex than previous assumptions. Their shape was determined as polygonal with flat sides and shared wall called the inter-alveolar septum.[7]

Within the alveoli, there exist two distinct types of alveolar epithelial cells type I and type II pneumocytes. Type I pneumocytes envelop roughly 95% of the total alveolar surface, creating an ideal environment for efficient gas exchange. Type II pneumocytes play a crucial role in producing surfactant, a substance essential for reducing the impact of surface tension within the alveoli. Gas exchange occurs through type I epithelial cells, contributing to a collective surface area of approximately 130 square feet. These numerous alveoli are interspersed among capillaries, forming an interface between air and blood, crucial for efficient gas exchange. [1, 7]

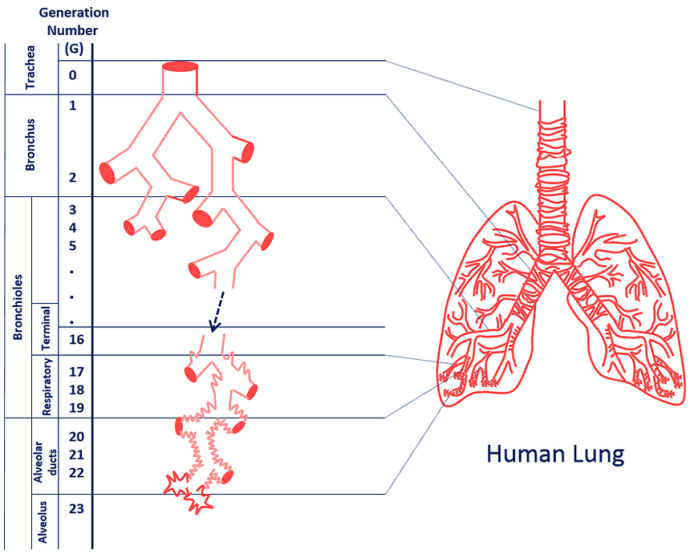

Fig. 1.3: Complex generation division from trachea, through main bronchus and bronchioles until alveolar region of alveolar ducts and alveolus [9].

1.2.3 Lungs

Most of this tracheobronchial tree is placed inside the lungs. Structurally the lungs are bordered by various bone or muscle structures, innervated by the nerve roots of C3, C4, and C5 via the phrenic nerve. The lung is enveloped in layers crucial for its function. The Visceral Pleura is the outermost layer covering the lung's surface. The Parietal Pleura lines the inner chest wall, diaphragm, and mediastinum, forming the pleural cavity along with the visceral pleura. This cavity is filled with pleural fluid, that minimizes friction during lung movement and facilitates smooth expansion and contraction within the thoracic cavity. [6]

The right and left lung anatomy are very similar. The right lung consists of three lobes, each is further divided into segments, each possessing its specific airway conduits. The upper lobe comprises three segments: apical, posterior, and anterior. The middle lobe includes lateral and medial segments and the lower lobe is divided into five segments: superior, medial, anterior, lateral, and posterior. [1]

In the left lung, the upper lobe contains the apical-posterior, anterior, inferior, and superior lingula segments, while the lower lobe contains the superior, antero-medial, lateral, and posterior basal segments. [1]

1.3 Relevant physiology parameters

Among many general physiological parameters like heart rate, blood pressure, body temperature, blood oxygen saturation, and others are some particularly important for the evaluation of the health of the respiratory tract.

1.3.1 Breathing frequency

Breathing frequency, also known as respiratory rate, is the number of inspirations per minute, given in breaths per minute. It's a vital physiological parameter used to assess respiratory health and function. In an average population, the value typically stands at approximately 12-18 breaths per minute during rest. Under increased workload, the value can escalate based on the intensity, reaching a maximum of about 40 breaths per minute. In trained individuals with increased lung capacity, the resting values may decrease to less than 10 breaths per minute, while maximum values can surge as high as 60 breaths per minute. Infants and children generally have higher normal respiratory rates than adults. [10]

1.3.2 Tidal volume

Tidal volume is the volume of air exhaled in one expiration or inspiration, given in liters. Average volume ranges between 500 to 700 milliliters during the rest of the general population. When under workload, values tend to rise in demand for more oxygen to meet the heightened metabolic needs, reaching levels up to 2.5 liters. Trained individuals may exhibit resting tidal volume increases of up to 1 liter or more. Under workload, these values can reach around 60% of the vital capacity, exceeding 4 liters. [10]

Some other important volume values, displayed in figure 1.4, are the inspiratory reserve volume of 3.3 liters for men and 1.9 liters for women and expiratory reserve volume of 1.1 liters for men and 0.7 liters for women, representing the volume that can be inhaled or exhaled after normal inhale or exhale. Next residual volume of 1.2 liters for men and 1.1 liters for women, which is the volume of air that stays in the lung after total exhalation and at the end forced expiratory volume meaning volume that can be exhaled in one second of maximum forced exhalation. This one is very dependent on the total respiratory state of each individual.

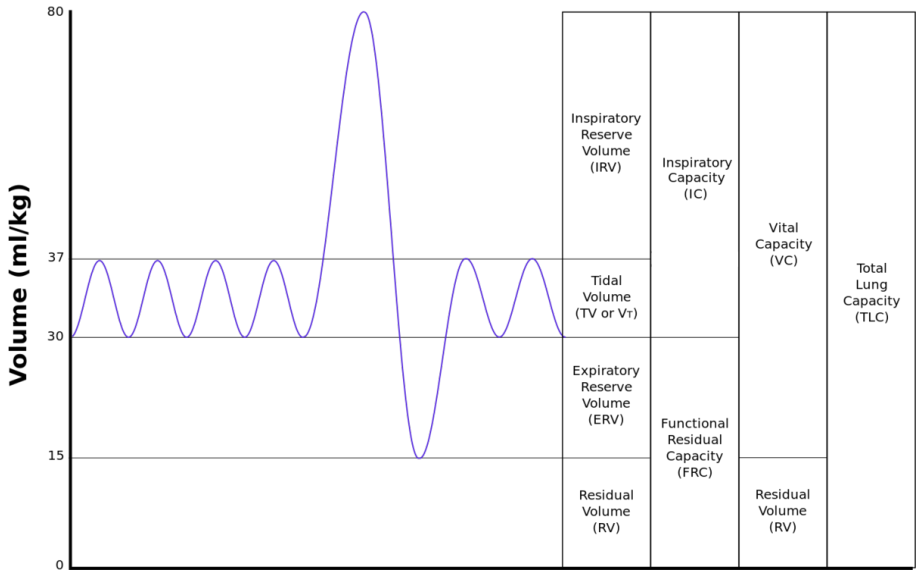

Fig. 1.4: Graphical representation of relevant volumes and capacities throughout the whole respiratory cycle [11].

1.3.3 Vital Capacity

Vital capacity is the maximum amount of air a person can exhale forcibly from the lungs after a maximum inspiration, given in liters. It is a static parameter influenced by factors like gender, age, fitness, etc., and averages around 3-4 liters in women

and 4-5.5 liters in men. After a low-intensity workload, vital capacity values might increase, necessitating breathing practice. Endurance training may augment vital capacity, potentially exceeding 6 liters. [10]

Other important lung capacities are an inspiratory capacity of 3.8 liters for men and 2.4 liters for women, which represents the total amount of air one can inhale. Next functional residual capacity represents the volume in the lungs at the end-expiratory position and its values are 2.4 liters for men and 1.8 liters for women. At the end the total lung capacity, meaning volume in the lungs after maximal inspiration. The values of total lung capacity are 6 liters for men and 4.2 liters for women.

1.3.4 Minute ventilation

Minute ventilation is the volume of air inhaled or exhaled from a person's lungs in one minute, given in liters per minute. It is calculated by multiplying breathing frequency and tidal volume, which typically amounts to approximately 10 liters per minute in both sporting and non-sporting individuals during rest. Under workload, ventilation increases, possibly reaching maximum values of around 120 liters per minute. Intense ventilation, surpassing 40-50 liters, often leads to mouth breathing. Endurance exercise can elevate ventilation significantly, up to 180 liters per minute. Minute ventilation is an essential parameter used to assess the overall efficiency of breathing. [10]

1.4 Common pathologies of the respiratory tract

Numerous factors can impact the organs and tissues comprising the respiratory system. Some originate from inhaling irritants found in the air, such as viruses or bacteria triggering infections, while others manifest due to aging or underlying diseases. Various conditions can provoke inflammation, swelling, or discomfort within the respiratory system.

1.4.1 Bronchial asthma

Bronchial asthma is a very common chronic respiratory condition characterized by chronic inflammation. The cause of this disease is determined as a combination of genetic and environmental factors. What is considered to be a big issue are allergens associated with urbanization. Inhaled allergens stimulate inflammatory reaction that inflicts airway hyperresponsiveness, obstruction, mucus hyper-production, and airway wall remodeling or thickening by epithelial transition. [12]

During an asthma attack, the muscles surrounding the airways tighten by the process of bronchoconstriction, the airway lining becomes swollen and inflamed, and excess mucus is produced, further narrowing the air passages. It is then difficult for air to move in and out, leading to the characteristic symptoms of asthma. [12]

Treatment aims to control symptoms, prevent exacerbations, and improve quality of life. This often involves a combination of medications, including bronchodilators to relax the airway muscles and corticosteroids to reduce inflammation. Inhaled medications are commonly used because they deliver the medication directly to the airways with fewer side effects compared to oral medications. [12]

Nebulizers are also used for either long-term or life-saving asthma treatment containing inhaled corticosteroids that help to reduce inflammation in the airways and reduce symptoms of breathlessness and chest tightness. Using a nebulizer to take your maintenance medication daily can help to prevent asthma symptoms from flaring up and asthma attacks from occurring. [15]

1.4.2 Chronic obstructive pulmonary disease

COPD is a progressive respiratory condition characterized by persistent airflow limitation in the lungs. It encompasses a group of lung diseases, primarily chronic bronchitis, and emphysema, which are often caused by long-term exposure to irritating gases or particulate matter, most commonly from cigarette smoke. It is a leading cause of morbidity and mortality worldwide, with symptoms typically worsening over time. The main symptoms include coughing, wheezing, shortness of breath, and chest tightness. [13]

Treatment aims to relieve symptoms, slow disease progression, and improve overall lung function and quality of life. Smoking cessation is the single most effective intervention to slow the progression of COPD and reduce symptoms. Other treatments may include bronchodilators to relax the airway muscles and improve airflow, corticosteroids to reduce inflammation, pulmonary rehabilitation programs to enhance exercise capacity and breathing techniques, oxygen therapy for severe cases with low blood oxygen levels, and vaccinations to prevent respiratory infections. [13]

COPD management often involves daily nebulizer therapy combining corticosteroids, anticholinergics, and beta-agonists, offering a convenient method to administer these medications together and effectively alleviate symptoms, leading to notable enhancements in quality of life. [15]

1.4.3 Cystic fibrosis

CF is a genetic disorder that affects multiple organ systems and exhibits a range of clinical problems of varying severity. It is caused by mutations in the CFTR gene, which leads to the production of thick and sticky mucus in various organs, particularly the lungs and pancreas. [14]

The primary cause of mortality in cystic fibrosis is pulmonary disease, where abnormal chloride transfer results in thickened mucus lining the airways, leading to chronic bacterial infections and inflammation, ultimately resulting in bronchitis, bronchiectasis, and respiratory failure, often complicated by hemoptysis and pneumothorax. Accompanying symptoms are persistent coughing, wheezing, shortness of breath, and frequent lung infections. [14]

CF is a chronic and progressive condition with no cure, but advances in treatment have significantly improved life expectancy and quality of life for people with CF. Treatment typically involves a combination of medications to thin mucus, improve lung function, prevent and treat infections, and aid digestion. Physical therapy techniques such as chest percussion and postural drainage are also commonly used to help clear mucus from the lungs. Managing CF often necessitates the simultaneous use of multiple inhaled medications, making a nebulizer an indispensable tool in treatment. CF patients typically require bronchodilators, hypertonic saline, steroids, and antibiotics, highlighting the importance of using a nebulizer that can be easily cleaned and disinfected due to their heightened susceptibility to germs. Vibrating mesh nebulizers, which lack complex components like tubes, are particularly suitable for this purpose. [14, 15]

1.4.4 Respiratory inflammation conditions

Respiratory infections encompass a variety of inflammatory conditions affecting the respiratory tract, commonly caused by viruses, bacteria, or fungi. They often present with symptoms such as coughing, congestion, fever, and difficulty breathing. Treatment typically involves antiviral or antibiotic medications depending on the cause, along with supportive care to alleviate symptoms. Preventive measures such as vaccination, good hygiene practices, and avoiding close contact with sick individuals can help reduce the risk of respiratory infections. For vulnerable groups like young children, pregnant women, the elderly, and immunocompromised individuals being at higher risk nebulizers offer a valuable treatment option as they efficiently deliver antibiotics directly to the lungs, aiding in rapid infection control. [15]

2 Medical aerosols in the human respiratory tract

The definition of aerosol is a dispersion of fine solid particles or liquid droplets in a gas . In the context of medicine, aerosols refer to tiny droplets or particles suspended in air, containing medications or therapeutic substances. They are generated to deliver medications directly into the respiratory system through inhalation [25].

2.1 Aerosol particles properties

Aerosols are categorized based on their origin. Those classified as primary originate directly in the atmosphere from natural sources like volcanic eruptions, sea spray, and erosion, as well as human-made sources such as industrial activities. Secondary aerosol particles form within the atmosphere through chemical reactions. Primary and secondary aerosols are characterized by the size, shape, and chemical content of the aerosol particles.

From a point of size, particles vary from diameters of a few nanometers to several tens of micrometers. A mixture of solid particles and liquid droplets in the air is called particulate matter (PM). Ultra fine particles usually marked as PM1 refer to those with a diameter smaller than 1 µm, fine particles referred to as PM2.5 with a diameter of less than 2.5 µm, whereas coarse particles, known as PM10, range between 2.5 and 10 µm [25]. The health effects of the particles are directly related to their size. Based on the size of particles, they can penetrate and deposit into different parts of the respiratory tract by different deposition mechanisms [26].

When discussing particle shape, the assumption often considers particles as spherical. This assumption serves as an idealized model essential for simplifying mathematical complexities concerning aerosol particle behavior. In reality, aerosols consist of irregularly shaped particles, leading to numerous challenges. [25]

The particle diameter can only be defined for smooth and spherical objects. For real-life particles, an equivalent diameter is defined using the concept of equivalent spheres. The size of the particle is determined by comparison to the equivalent sphere with same properties and behaviour as the actual particle. Different measurement technique use different measuring equivalents. The most common are sphere of same maximum or minimum length, volume, weight, surface area or sedimentation time. [27].

Optical equivalents are used for optical measurement methods. The laser diffraction equivalent diameter represents the size of a sphere that produces an identical diffraction pattern to that of the particle, given the same detector setup.

Aerodynamic diameter refers to a theoretical measurement used to describe the behavior of aerosol particles in the gas. It refers to a sphere particle with a density of 1 g/cm^3 (equivalent to water density), with the same inertial properties as the actual particle. This way particles with different physical diameters might have similar aerodynamic diameters. [26]

Based on this study [28] underlining the importance of correct comparison of optical equivalent diameter measured by optical methods and generally descriptive aerodynamic diameter, a quadratic equation can be used to convert there diameters between each other.

$$D_{ae} = -0.0045 * {D_{op}}^2 + 1.0603 * D_{op} + 0.4513 \tag{2.1}$$

2.2 Aerosol deposition in the human respiratory tract

Medical aerosol deposition within the human respiratory tract is a complex process influenced by various factors including particle size, inhalation technique, respiratory anatomy, airflow dynamics, and deposition mechanisms.

Factors such as breath-hold duration, inhalation flow rate, and coordination between device actuation and inhalation greatly influence the distribution of aerosols. Variations such as airway bifurcations and narrowing, in airway geometry, can lead to uneven distribution of aerosols. Turbulent airflow patterns in the upper airways enhance particle deposition through impaction, while laminar flow in the smaller airways facilitates particle penetration and distribution. [29]

Particle size significantly influences the deposition pattern within the respiratory tract. Larger aerosol particles, typically greater than 5 micrometers in diameter, primarily deposit through inertial impaction and gravitational settling in the upper and larger airways, such as the nasal cavity, pharynx, larynx, trachea, and bronchi. These regions experience significant changes in airflow direction and velocity, facilitating particle deposition.

Coarse particles smaller than 3 micrometers undergo deposition mainly in the smaller airways of the pharynx, larynx, trachea, and bronchial region, where airflow patterns lead to turbulent dispersion and increased chances of particle impaction. Particles ranging between 0.3 and 3 micrometers in diameter deposit in areas characterized by smaller flow velocities, primarily due to gravitational settling. In contrast, particles smaller than 0.3 micrometers deposit predominantly by diffusion in the alveolar region, where airflow velocities are minimal, and the surface area for particle interaction is maximized.

The deposition pattern depicted in Figure 2.1 illustrates the areas of probable deposition within the respiratory tract based on the diameter of deposited particles. [30]

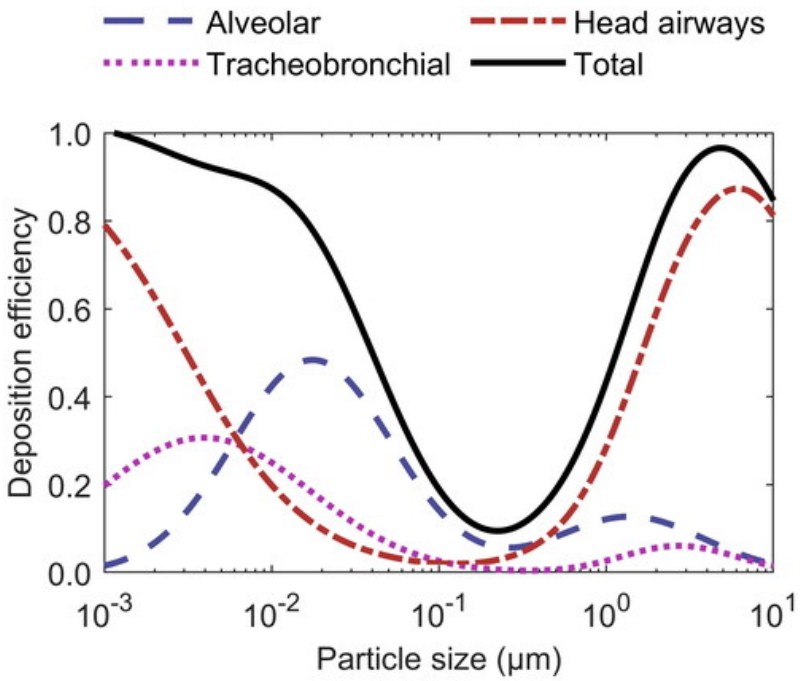

Fig. 2.1: Particle deposition in the respiratory tract based on their diameter [31].

2.2.1 Deposition mechanisms

The effectiveness of inhalation therapy relies not just on the properties of the drugs, but also on where and how much of the medication is deposited within the respiratory tract. By thoroughly exploring the deposition mechanism displayed in the figure 2.2 a very high precision in effective delivery can be achieved. It makes this inhalation therapy very targeted, both for maximizing the therapeutic effect and minimizing side effect costs.

Inertial Impaction

Inertial impaction is the main deposition mechanism for particles larger than 5 µm and it is due to their inability to follow sudden changes in the gas flow direction. Particles deviate from the flow direction because of their momentum and get caught up in the wall. As the particle size gets higher, the probability of deposition by inertial impaction gets also higher. This probability is expressed by Stokes number defined by particle diameter d_p and density of the particle ρ_p, velocity u and dynamic viscosity μ of the carrier gas, and diameter of the airway d. [29]

$$Stk = \frac{\rho_p d_p^2 u}{18\mu d} \tag{2.2}$$

Turbulent mixing

The large airways and upper respiratory tract are also influenced by turbulent mixing. It is a mechanism of deposition that refers to irregular fluctuations or blending experienced by the fluid in turbulent conditions. These fluctuations result in constant alterations in fluid velocity causing particles to shift in both magnitude and direction. [29]

Interception

Aerosol deposition by interception occurs when inhaled particles, particularly prolonged-shaped ones (typically fibers), travel close to the surface of the airway and adhere to the walls of the airways during inhalation when the particle touches the surface. [29]

Gravitational sedimentation

For quite a wide range of particle size from 1 to 8 µm is gravitational sedimentation possible deposition mechanism. It takes place mainly in the parts of the tract where the diameter is rather small like the small airways and alveolar cavities. The Settling velocity of the particle is expressed by the coefficient of gravitational sedimentation computed with particle diameter d_p, particle density ρ_p, gravitational acceleration g and dynamic viscosity μ. This mechanism of deposition, the same as inertial impaction, also increases with the rising size of particles. [29]

$$V_S = \frac{\rho_p d_p^2}{18\mu} g \tag{2.3}$$

Brownian diffusion

The deposition mechanism of Brownian diffusion is most typical for the smallest particle sizes lesser than 0.5 µm. It results from the random motions of the particles caused by their collisions with gas molecules. Shows maximum effectiveness within the acinar region of the lung due to the notably reduced air velocities. As the only one increases its effect with decreasing size of the particles. Brownian diffusion coefficient describes the mechanism using Boltzman constant k, absolute temperature T, and Cunningham's correction factor c in addition to particle diameter d_p and dynamic viscosity μ. [29]

$$D_B = \frac{ckT}{3\pi\mu d_p} \tag{2.4}$$

Electrostatic precipitation

Electrically charged particles near airway surfaces cause the generation of image charges on these surfaces. This electrical charge then leads to an electrostatic pull, attracting the particles towards the airway walls. [29]

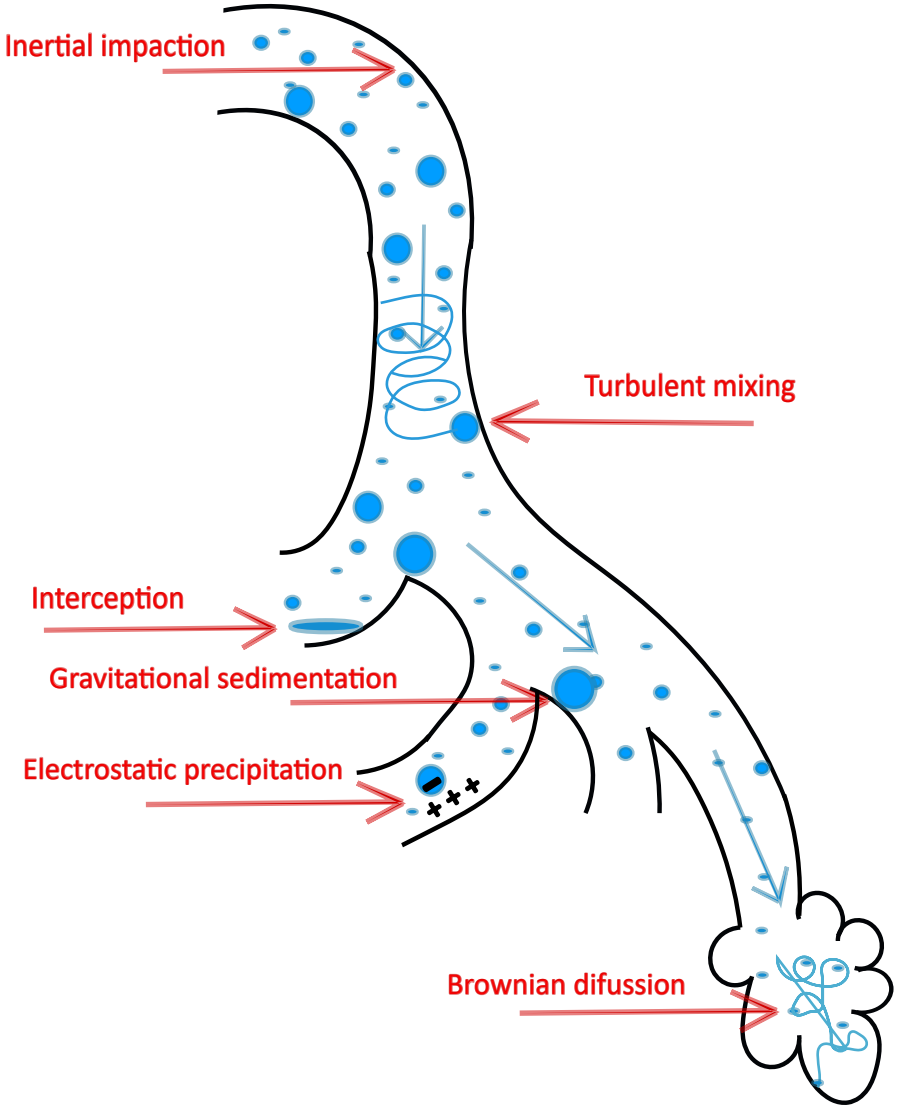

Fig. 2.2: Different deposition mechanisms: interception, inertial impaction, turbulent mixing, gravitational sedimentation, electrostatic precipitation and brownian difussion present in the different parts of the human respiratory tract.

3 Production and measurement of medical aerosols

Aerosol inhalation for drug delivery is a widely recognized and firmly established method for managing various pulmonary diseases. This mode of administration offers substantial advantages compared to oral and intravenous routes. By leveraging the lungs' exceptional capacity for local and systemic non-invasive drug administration, it optimizes therapeutic efficacy.[16]

The lungs, with their expansive surface area, coupled with a thin air-blood barrier facilitate the rapid absorption of medications used for local therapies. This setup allows for achieving high concentrations of drugs in the targeted lung tissues while minimizing systemic side effects. This approach allows for the effective use of smaller doses while potentially reducing systemic side effects. There is a large number of available nebulizers on the market and their design is what determines the aerosol particle size and nebulizer output, by which they are chosen for different respiratory problems. Four common types of aerosol generators are used for inhalation drug delivery: pressurized metered-dose inhalers, soft mist inhalers, dry-powder inhalers, and small-volume nebulizers.[16]

3.1 Pressurized metered-dose inhalers

These aerosol production devices were established in 1950 but they remain a secure option for treating pulmonary diseases. The pressurized metered-dose inhaler is a compact, self-contained drug delivery device capable of dispensing multiple doses through metered values. The key components of the pMDI device are a canister, which contains the medication in a liquid form along with the propellant that creates pressure within this canister, an actuator, which ensures a precise dose release when the patient presses down the canister and a mouthpiece, which allows the proper inhalation of aerosolized medication. Correct use of a pMDI requires coordination between pressing the canister and inhaling slowly and deeply. [17]

3.2 Soft mist inhalers

Soft mist inhalers (SMI) are low-velocity, propellant-free multidose spray devices designed to deliver medication to the respiratory system in the form of a fine mist. Their ability to generate a slow-moving and soft mist allows a comfortable and effective inhalation, which makes them particularly well-suited for individuals who

may have difficulty using other inhalation devices, such as young children, elderly patients, or those with certain physical limitations. [18]

3.3 Dry-powder inhalers

Dry-powder inhaler (DPI) serves as an aerosol device that administers drugs in powdered form, typically integrating a breath-actuated dosing system for delivery. Unlike pressurized metered-dose inhalers that deliver a measured dose of medication as an aerosol spray, dry-powder inhalers release a dry powder for inhalation. The medication in a DPI is stored in the form of a dry powder within the inhaler device. Because it is a breath-actuated device, it releases the medication when the patient inhales through the inhaler. Some dry-powder inhalers use a reservoir containing the powdered medication, while others require individual medication capsules that the user loads into the device before each use. They do not need a propellant to disperse the medication. [19]

3.4 Medical nebulizers

A medical nebulizer is a propellant-free device used to administer medication in the form of an aerosol directly into the respiratory tract. It's commonly used to deliver medications for respiratory conditions like asthma, chronic obstructive pulmonary disease, cystic fibrosis, and other critical illnesses. The process involves placing the liquid medication into the nebulizers' chamber. As the device operates, whether through compressed air, ultrasonic vibrations, or mesh vibration, it aerosolizes the medication and creates a mist. The patient then inhales this mist through a mouthpiece or a mask fitted over their nose and mouth.

A nebulizer's purpose is to deliver medications in aerosolized form to the terminal alveoli in the lungs. Their efficiency relies on two key factors: the emitted dose of the drug and the fine particle fraction. These parameters together determine how effectively the medication is delivered. When a solution is nebulized, the size and shape of the particles, known as the mass median aerodynamic diameter, play a crucial role in determining where in the airways the drug is deposited. Larger particles (>5µm) can not travel beyond the upper airways (oropharynx and mouth), while medium-sized particles (2-5µm) are deposited in the central airways. Only the fine particles (<2µm) can successfully reach the alveoli, where optimal drug absorption takes place. [16]

The main general diffrances between devices most commonly used for inhalation therapy are listed in the following table 3.1.

Tab. 3.1: Inhaler devices comparison.

Feature	pMDIs	SMIs	DPIs	Nebulizers
Propellant	Propellant-driven	Propellant-driven	Propellant-free	Propellant-free
Activation mechanisms	Coordination of inhalation and accutation	Acutated by breathing in	Forceful inhalation	Powered by electricity or compressed air
Aerosol characteristics	Fine aerosol particles	Larger droplets	Dry powder	Fine mist
Dose counter	Available in some models accutation	Available in some models accutation	Available in some models accutation	Not applicable
Cleaning	Regular cleaning required	No cleaning required	No cleaning required	Regular cleaning required

3.4.1 Jet nebulizers

Traditionally, jet nebulizers are the oldest and clinically most used type of nebulizer for the treatment of pulmonary diseases. They operate on working principle described in figure 3.1 by utilizing compressed gas sourced from a cylinder, hospital airline, or an electrical compressor to transform a liquid substance into an aerosol. This transformation occurs thanks to high-velocity gas (2-10 l/min) directed tangentially or co-axially through a narrow nozzle. At the point where the air jet exits, a region of negative pressure forms, inducing the liquid from a reservoir to be drawn up a feed tube by the Bernoulli effect. As the liquid emerges it collapses into fine droplets. Baffles inside the medication chamber filter out sizable aerosol droplets, sending them back into the jet for reuse. This process leads to the repeated circulation of some medication within the nebulizer. Although this could potentially affect the integrity of certain drugs, the baffle effectively screens out larger droplets, ensuring that the aerosol emitted by the device is appropriately sized for effective lung delivery. [20, 21]

The advantage above pMDIs and DPIs is in delivering some formulas, that these mentioned devices cannot. On the other hand, the need for compressed gas is a disadvantage, that requires the development of newest, more effective technologies. To reduce drug wastage and damage, four technology categories of jet nebulizers have been invented. Jet nebulizers with a corrugated tube generate continuous aerosol throughout the breathing cycle but suffer from significant drug loss during expiration. A jet nebulizer with a collection bag releases aerosol only during inhalation,

storing aerosols generated during expiration for subsequent inhalation through a one-way valve, offering advantages over nebulizers with corrugated tubing by reducing drug escape into the environment and enhancing aerosol drug delivery to patients' lungs. Breath-enhanced jet nebulizers release aerosol predominantly during inhalation via one-way valves in the mouthpiece and breath-actuated jet nebulizers minimize drug wastage by delivering aerosol exclusively during inspiration. [20]

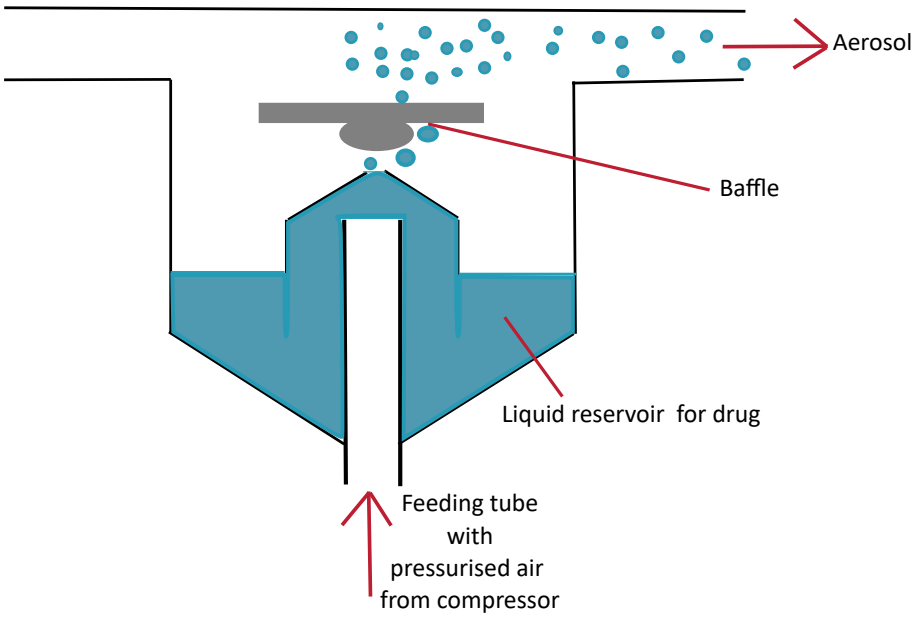

Fig. 3.1: Working principles of a jet nebulizer, that utiliaze compressed air through cylinder and buffer element to create droplets of aerosol.

3.4.2 Ultrasonic nebulizers

Ultrasonic nebulizers from the figure 3.2 are compressor-free and usually run via battery. The working principle revolves around the utilization of ultrasonic vibrations. When an electrical current is applied, the piezoelectric element generates vibrations, typically oscillating at frequencies around 1-3 MHz. The piezoelectric crystals' base is held in place firmly, transmitting vibrations from its frontal surface to the fluid. These created ultrasonic waves travel through the liquid in the reservoir and induce vibrations that break the liquid into droplets, forming a fine aerosol mist. Ultrasonic nebulizers are known for their efficiency in producing a fine mist and they are generally quieter than other types. On the other hand, the created vibrations tend to create heat, which is damaging to the inhalation substance. [21, 22]

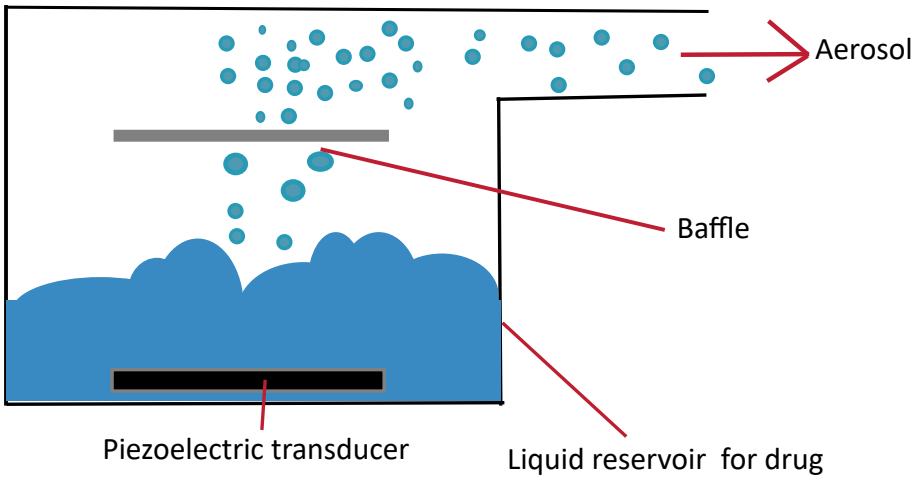

Fig. 3.2: Working principle of an ultrasonic nebulizer using vibrations from piezoelectric element on creating of small aerosol doplets.

3.4.3 Mesh nebulizers

Compared to traditional jet and ultrasonic nebulizers, the introduction of vibrating mesh nebulizers represents a significant advancement. They are also compressor-free devices plus they successfully correct the overheating problem of ultrasonic nebulizers. They might be either active or passive. Active devices create vibration with a piezoelectric element when a current is introduced. This up-and-down movement of the element causes the liquid to pass through the fine holes in the mesh shown in the figure 3.3 producing aerosol. [20]

Passive devices operate by employing a perforated plate containing 6000 3 µm sized tapered holes. Vibrations originating from a piezoelectric crystal are transferred to this perforated plate. These passive vibrations within the plate cause the extrusion of liquid through the holes. The missing baffle reduced the probability of drug damage. To further improve drug delivery, some mesh nebulizers are also manufactured as breath-activated, enabling stopping the aerosol production when exhalation. [20]

Another technical design for mesh nebulizers incorporates smart nebulizer technology, that is utilizing adaptive aerosol delivery (AAD®) technology by analyzing the patient's breathing pattern to optimize aerosol drug delivery during inhalation while reducing aerosol losses during expiration. It minimizes variation in drug delivery, improves patient adherence to treatment, and offers feedback on device effectiveness, thereby enhancing control over drug doses and deposition in the lungs. [20]

Several advantages are introduced including shorter treatment durations, minimized drug wastage, and enhanced delivery of medication directly to the lungs.

These qualities make them particularly suitable for administering expensive novel inhaled therapies. However, these performance benefits come with a higher initial cost for the device. Additionally, mesh nebulizers may encounter difficulties in aerosolizing highly viscous or crystallizing solutions, often leading to micro-aperture blockages [20, 21]. In some studies, equal drug delivery was demonstrated between mesh and ultrasonic nebulizers [23] and more efficient drug delivery from mesh than jet nebulizers [24].

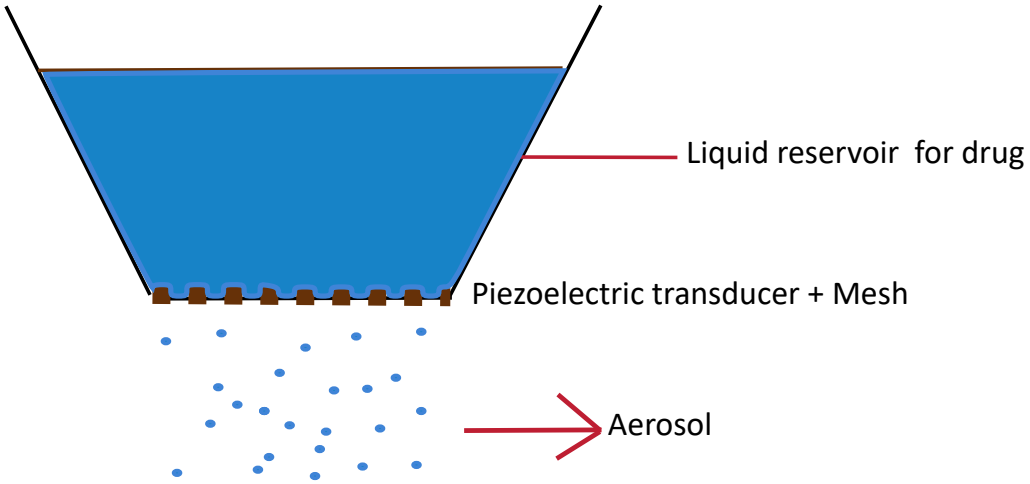

Fig. 3.3: Working principles of a mesh nebulizer that generates aerosol droplets by vibrations created by piezoelectric element and mesh placed near by.

Tab. 3.2: General characteristics of nebulizer types.

Type	Conventional jet	Ultrasonic	Vibrating mesh
Power	gas-driven	electricity-driven	batteries-driven
Particle size [µm]	4-7	4-7	3-5
Residual volume [ml]	1-1.5	1-1.5	0.1-0.5
Treatment time [min]	10-20	5-15	5_10
Output rate [ml/min]	0.1-0.5	0.1-1	0.1-1.5

3.4.4 Particle deposition measurements

In inhalation therapy, only a portion of the inhaled dose effectively reaches the target area. The investigation into the quantity of drug deposition leads to understanding how to correctly optimize the delivery devices to achieve the highest efficiency in this way of drug administration.

Several pharmaceutical models can predict the amount of deposition, based on well-studied deposition mechanisms, but they have a limited accuracy. Thanks to the complex nature of this task, computations in these models require simplification that lowers their accuracy. [30]

Scanning Mobility Particle sizer

The Scanning Mobility Particle Sizer (SMPS) sorts charged particles based on their mobility in an electric field. After neutralization, particles pass through a Differential Mobility Analyzer to select a specific range by electrical mobility. These chosen particles are counted for concentration in a Condensation Particle Counter. [30, 32]

Condensation particle counter

A condensation particle counter (CPC) operates by measuring the number concentration of aerosol particles in the air. It works by introducing the aerosol sample into a supersaturated vapor within the instrument, when the aerosol particles come into contact with the supersaturated vapor, they act as nuclei for condensation, causing the vapor to condense around them, forming droplets. These droplets grow larger as they continue to collide and merge with other droplets. The resulting enlarged particles are then counted using optical or electrical detection methods, providing a precise measurement of the number of aerosol particles present in the sampled air, typically within a specific size range. [30, 33]

Radioactive techniques

Radioactive techniques for measuring aerosol deposition in the respiratory tract include using radioactive tracers like Technetium-99m or Xenon-133, which label aerosol particles or gases for tracking. Radiolabeled particles enable tracking deposition, detected by gamma counters or autoradiography. Gamma scintigraphy and Positron Emission Tomography (PET) use inhaled radiolabeled aerosols to visualize deposition patterns in the lungs through gamma rays or positron-emitting isotopes. These techniques offer detailed insights but require safety measures due to radiation exposure risks. [30, 34]

Gravimetric analysis of filters

Filtration and gravimetric analysis, the oldest and most commonly employed method, are used to gather ambient concentrations of suspended particulate matter. In this method, air passes through a filter that collects particles. The filter is weighed before and after sampling, and the difference determines the mass of deposited particles. This method provides a straightforward measure of total particle mass deposited on the filter but may not differentiate between particle types or sizes. [30, 35]

Electron microscopy

By using electron microscopy and energy-dispersive X-rays a characterization of individual aerosol particles, their sizes, shapes, and distribution can be obtained. After collecting samples, for example from a filter, they are usually prepared by coating with some conductive material or frozen for later examination. This is a high-resolution technique enabling not only characterization but also visualization of deposited aerosol particles. [30, 36]

Thermal precipitator

A thermal precipitator works by exposing a gas stream containing suspended particles to high temperatures. This heat causes particles to agglomerate and deposit onto collection surfaces within the device. As particles gain thermal energy, they lose suspension properties and settle out onto these surfaces, allowing cleaned gas to exit the precipitator. [30, 37]

Impingers

An impinger operates by directing particle-laden air through nozzles into a liquid-filled chamber, where particles are collected. The distance from the nozzles to the liquid and the airflow rate determines the size of the particles collected. The liquid prevents particle desiccation, but turbulence from the airflow may affect particle viability. However, factors like evaporation, re-aerosolization, and particle adherence to chamber walls can also impact the impinger's effectiveness. [30, 38]

Spectrometry

An optical aerosol spectrometer uses laser light to interact with aerosol particles in the air. It detects the scattered or diffracted light from these particles and analyzes its intensity and patterns. By interpreting this data, the spectrometer provides information about particle size distribution, concentration, and sometimes composition in the sampled air. [30, 39]

4 Materials and methods

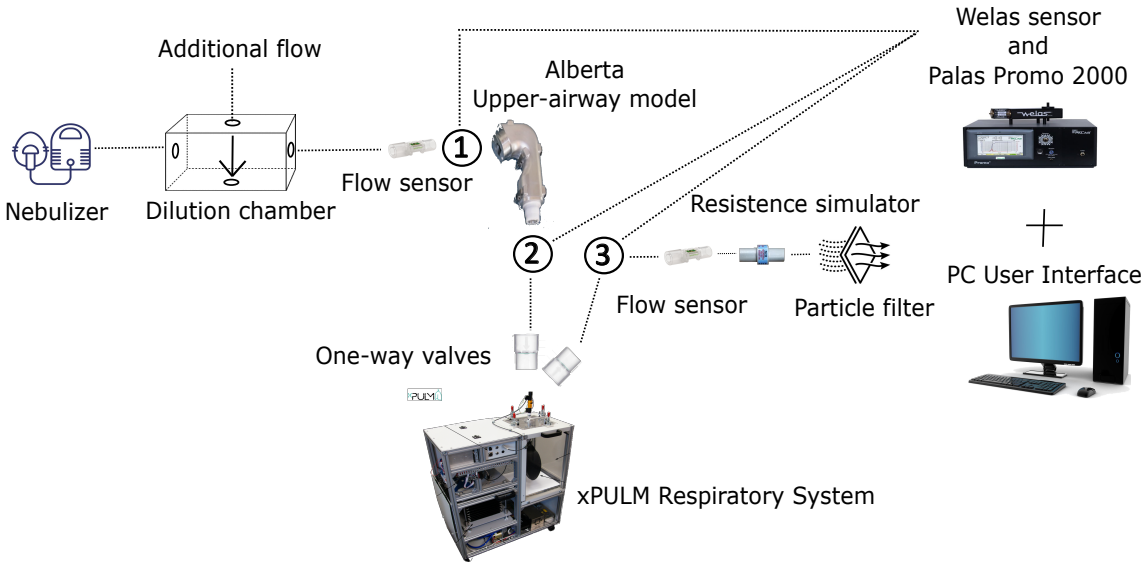

Fig. 4.1: The designed experimental measurement setup.

4.1 Measurement setup

The designed aerosol measurement setup displayed in the figure 4.1 contained nebulizers as a source of aerosol, the dilution chamber with the additional flow, the connection tubing and 3D printed connectors between the components, sensirion flow sensors, the idealized mechanical upper-airway model Alberta, Cosina one-way valves, the xPULM electro-mechanical respiratory simulator, sampling points (1,2,3) connected to the wellas sensor 2200 and the optical aerosol spectrometer Palas Promo 2000 with setted flow of 5 liters per minute. All measurements were dispalyed and analyzed in the User Interface PDAnalyzer on the Computer.

4.1.1 Source of aerosol

In this study evaluating medical aerosol delivery, a comprehensive examination of three distinct nebulizer devices was conducted, each representing different technologies and intended applications, including jet, ultrasonic, and mesh nebulizers.

The Medisana Inhalator IN 500 Compact is a representation of a jet nebulizer subjected to testing. It relies on a standard electrical network for power, operating at 230 V. Operating on a jet flow of 4-7 l/min offers an aerosol output rate of 0.2 ml/min and a maximum filling volume of 10 ml. Its particle size distribution, with

particles primarily under 5 µm, makes it suitable for targeted respiratory therapy, enhancing its usability and convenience. [40]

In contrast to the jet nebulizer, the Dittman Inhaler IHG 375 represents the ultrasonic technology, featuring an ultrasound frequency of 140 kHz. This device caters to treating respiratory illnesses affecting the upper respiratory tract, such as asthma or allergies. With an aerosol output rate of 0.25 ml/min and a mass median diameter of below 5 µm, it offers precise medication delivery. Operating on either two AA batteries or a 3V power supply unit, it provides flexibility in usage scenarios. Patients are advised to utilize slow, deep breaths during treatment to facilitate optimal aerosol dispersion within the bronchial tubes, followed by normal exhalation for efficient medication uptake. [41]

Finally, the Omron U100 Microair, representing vibrating mesh nebulizers, was evaluated as a battery-powered alternative. With an estimated mass median aerodynamic diameter of 4.5 µm, it ensures effective aerosol distribution. Offering an aerosol output rate of 0.1 ml/min, it delivers medication efficiently while affording portability and convenience. Its maximum filling volume of 10 ml further enhances its usability. [42]

Fig. 4.2: Evaluated nebulizer devices. (A) Medisana jet nebulizer. (B) Dittman ultrasonic nebulizer. (C) Omron vibrating mesh nebulizer.

Tab. 4.1: Comparison of properties of used nebulizers.

Name	Medisana Inhalator IN 500 Compact	Dittman Inhaler IHG 350	Omron U100 Microair
Type	jet	ultrasonic	mesh
MMAD [µm]	<5	<5	<4.5
Aerosol output rate [ml/min]	0.2	0.25	0.1
Fill volume [ml]	10	8	10

4.1.2 Dilution chamber

Throughout the testing measurements, it was discovered that the aerosol generated from tested nebulizers was very concentrated resulting in inaccurate measurements. A glass chamber with controllable openings was incorporated between the nebulizers and the input of the representation of the respiratory tract. An additional flow of approximately 50 liters per minute was connected from the external flow source to further dilute the aerosol solution.

4.1.3 Respiratory tract representation

The upper airways are represented by the Alberta upper-airway model (AUAM), which is an idealized model of upper airways, that comes out of extensive research, academic literature, and also CT and MRI scans. The precision of this model is ensured by averaging living subjects' anatomy, creating a perfect reproducible human-like geometry. Despite its relative simplicity compared to the actual human throat, the geometry can reliably mimic the aerosol motion in the human throat. The model contains 4 regions representing the oral cavity, the pharynx, the epiglottis, and the larynx. It is chemically compatible with a wide range of medications to be tested. It is a great option to measure the in vivo behavior of inhaled substances. [43]

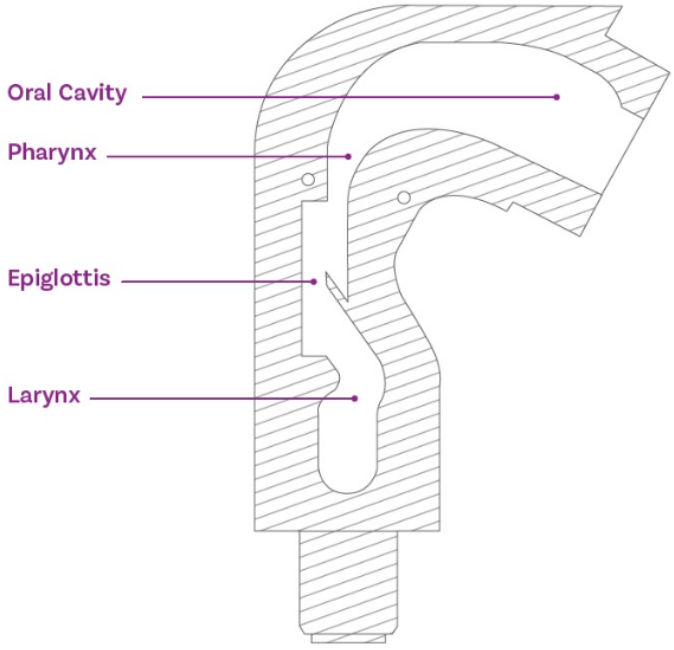

Fig. 4.3: Scheme of the Idealised upper-airway Alberta model [43].

To represent human lungs in this experiment, either polymer bags or porcine lungs were used. They are widely utilized in many biomedical researches due to their very similar anatomy, which makes this compensation very effective. Although there are some differences, the porcine trachea is longer and more cartilaginous, the broncho-tracheal tree has a similar number of bronchial generations and the average length of the perinatal porcine acinus is shorter compared to humans, 5 mm against 11 mm. Both human and porcine left lung consist of 2 lobes. In contrast to the human right lung, which has three lobes, the porcine right lung is divided into four lobes. [47]

For breathing simulations throughout the measurements an electromechanical lung simulator xPULM™ was used. It is a sophisticated device designed to replicate the complex mechanics of human breathing. The simulator offers various functionalities. These include performing breathing simulations with customizable flow profiles, adaptability of simulation parameters such as frequency and tidal volume, and the interchangeability of lung equivalents. The construction of the simulator is inspired by the functionality of the human respiratory system, integrating analogies between its main components and functional elements of the respiratory system. The thoracic chamber as the central part of the setup contains the some lung equivalent and monitoring sensors for pressure, temperature, and humidity. The respiratory drive system contains a motor and mimics diaphragmatic and intercostal muscle movements during breathing. Real-time control of simulation parameters is facilitated by embedded LabVIEW processing, ensuring dynamic adaptation to condition changes. [44]

Fig. 4.4: Electromechanical Lung Simulator xPULM™ [44].

4.1.4 One-way valves

To secure the separation of inhaled and exhaled air, one-way valves from Qosina were utilized. These one-way respiratory valves with a 22 mm (inner diameter) outlet and 22 mm (outer diameter) inlet provide a directional flow of gases and air. The membrane allowing the one-directional flow is from silicone and in the testing measurements was found not sufficient enough and it was replaced with a thinner latex membrane. [45]

4.1.5 Flow sensors

For measuring the flow in the experimental setup, the SFM3300 mass flow meter was used. It is a sensor for proximal flow measurement in respiratory applications such as ventilation or anesthesia. It measures bidirectional flow volumes of up to 250 slm. Additionally, the sensor is equipped with medical cones of 22 mm for pneumatic connections, along with a mechanical interface to facilitate user-friendly electrical connectivity. [46]

4.1.6 3D printed connections

All utilized components were connected through connectors that were designed in the 3D EXPERIENCE SOLIDWORKS® software, prepared and sliced in the UltiMaker Cura, and printed out from health-save PLA filaments on the Ultimaker 2+ Connect the 3D printer. The connectors composition is displayed in the figure 4.5. The connection tube leading from the dilution chamber to the representation of the respiratory tract was connected to the flow sensor through the printed component (1). The flow sensor was connected through the top connector (2) to the input of the AUAM representing the initial part of the respiratory tract representation. The output of the AUAM was connected to a connector complex (4, 5, 7), that contained a connection for AUAM (4), one-way valves (6) to separate inhaled and exhaled air, a connection to the xPULM breathing simulator (5) and connection to another flow sensor (7).

Firstly, the materials for printing the connections were considered. The connectors should be biocompatible, inert, and non-reactive to aerosol or additional experimental substances. Any potential interaction or leaching could introduce confounding factors compromising its validity. PLA meets all these requirements.

Subsequently, when considering the shape of all connectors, losses, and dead space in the aperture were taken into consideration. They were modeled to minimize these aspects and smoothed where possible. When plastic material meets another plastic or metal, a canal for a rubber band was incorporated to prevent any leakage.

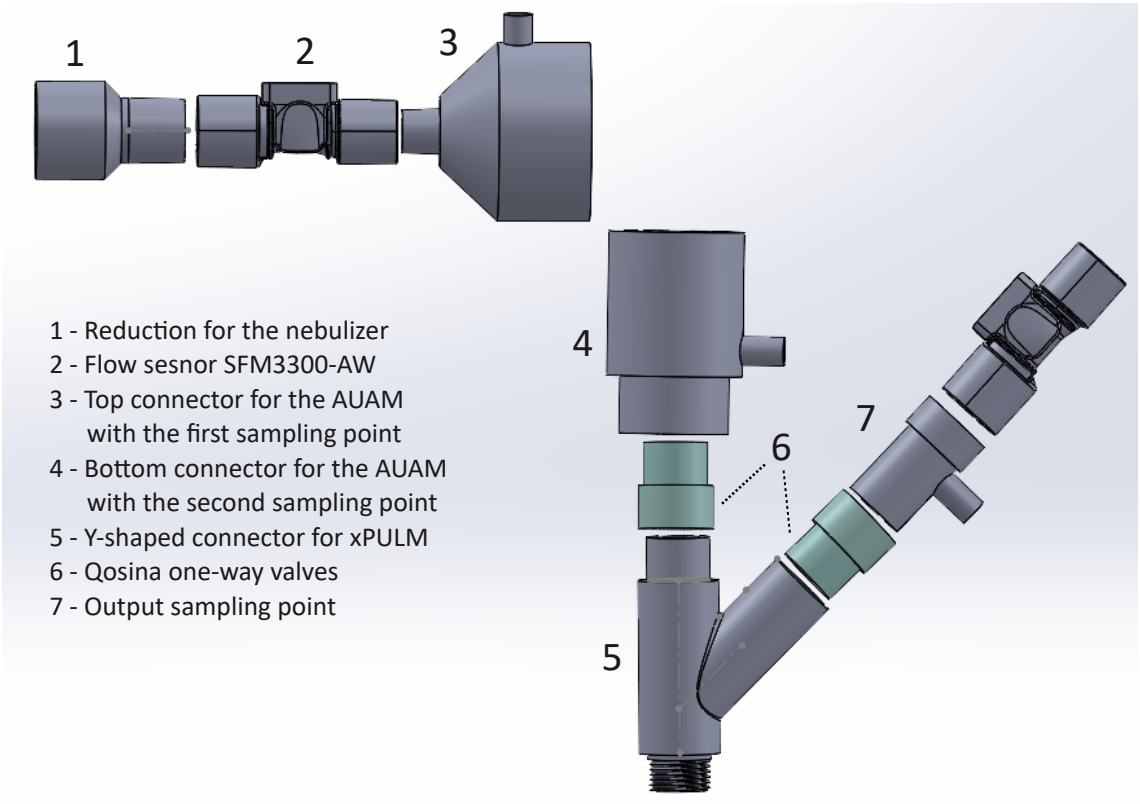

Fig. 4.5: Complex setup of connectors for the measurement setup containg 3D printed PLA connections, two flow sensors, two one-way valves and 3 sampling points.

4.1.7 Optical aerosol spectrometer

Palas Promo 2000 is a concrete type of spectrometer used in the following measurement. By operation principle, it is a light-scattering aerosol spectrometer designed for particle size analysis and concentration determination. In optical particle measurement, a light wave from a light source is re-directed by the phenomenon of refraction, reflection, and diffraction at small particles. It is based on the Mie theory of light scattering for particles with a size similar to the size of the wavelength. Each particle is illuminated by a white light and each scattered signal is detected at an angle of 90°. All detected signals are counted and create information about the aerosol number concentration. By the Mie theory, the duration of the scattered light signal is directly proportional to the particle size. Even intensity distribution of light inside the measurement volume is achieved by the usage of the white light and very small measuring volume that is defined optically. [48]

The measurement range for the number concentration is from 1 to 16^4 particles/cm^3. The range for measurable particle size is from 0.2 to 10 µm, due to the usage of the welas sensor 2200 and it is also a target size range for respirable particles. It is

compatible with welas sensors and features innovative light wave conductor technology. Welas® sensors come in different measurement volumes and the Promo® 2000 can seamlessly connect via fiber optic cables. Based on specific measurement needs, different sensors enable different particle size categories. The device operates with 128 channels per measuring range which ensures a high particle size resolution and classification accuracy. [48]

An advantage of using specifically this spectrometer lies in its patented T-shaped aperture, which ensures minimalization of coincidental events and border zone errors. It is designed to be selectively sensitive to scattering events along a specific direction so that certain scattering angles can be emphasized and others suppressed. This aperture contains two T-shaped quadrants with determined optical measuring volume. The size of a particle can be precisely determined only when it crosses both volumes. The scattered light is connected via optical fibers and leads to the evaluation unit [48]. Another important advantage is that the measurement takes place in real time, so the changes in particle size and concentration are visible throughout the whole process of the breathing simulation. One of the limitations of the Promo 2000 Spectrometer is the lower threshold for small particle size detection. Particles smaller than 0.5 µm are better measured by different measurement techniques.

Between biggest advantages of optical spectrometers belong the possibility to measure the aerosol directly and right away read the results and the ability to conduct multiple measurements in a row.

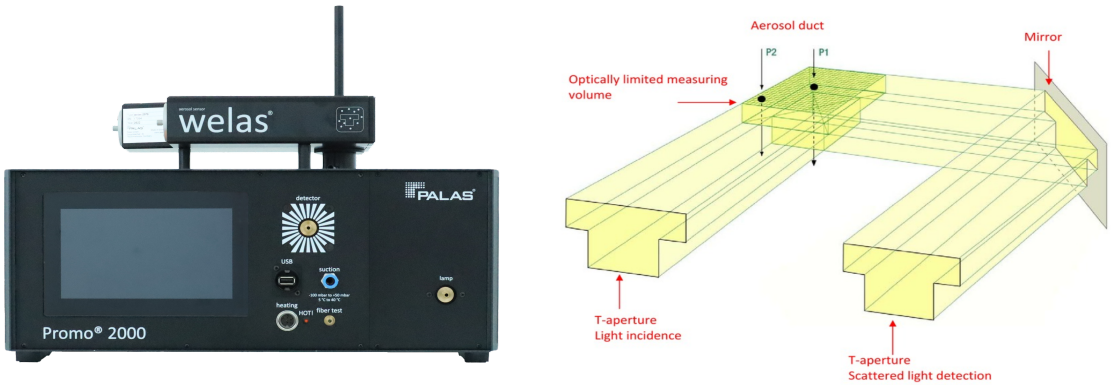

Fig. 4.6: On the left: Palas Promo 2000 spectrometer device with Welas sensor 2200 on the top and on the right: patented T-shaped aperture technology of the Promo 2000 device [48].

4.2 Measurement methods

The methods are derived from current standards (ISO 27427:2023) and reviewed studies concerning aerosol deposition in the human respiratory tract [30, 49, 50, 51].

The ISO 27427 standard was developed based on the general European Standard from 2001 to 2010 and optimized a few times since then. The main limitations it focuses on are replacing a constant value of flow with complex varying flow and flow rate values derived from realistic breathing.

4.2.1 Breathing pattern determination

Determining the breathing pattern for the breathing simulator is a critical aspect. The breathing pattern chosen should closely mimic physiological respiratory cycles to ensure an accurate representation of real-world conditions. In both measurements, a simulation of physiological breathing is utilized. Breathing frequency was set to 15 breaths/min, the ratio between inhalation and exhalation was set as 1:1, and tidal volume to 500 milliliters. It is possible to change the values of these parameters or to monitor them while ongoing measurements in the LabVIEW interface operating the xPULM.

4.2.2 Measured parameters

Aerosol output and output rate

Values of aerosol output either in milliliters or in particles indicate the amount of aerosol generated by the aerosol source, in this case, a medical nebulizer. By following a set of rules like the same nebulization time and the same testing solution, the output of different medical nebulizers can be compared. The same applies to values of aerosol output rate.

Residual volume

Residual volume is a critical metric for assessing a nebulizer's effectiveness in medication delivery. The higher value of the percentage of used liquid volume indicates more efficient delivery of the medication.

Size distribution

One of the substantial factors determining the behavior of aerosol particles within the respiratory system is the size distribution of generated particles. A narrow size distribution, characterized by a concentration of particles around a specific diameter, enhances the likelihood of uniform deposition. In contrast, a broader size

distribution may result in particles being deposited across various regions of the respiratory tract.

Particle diameter

Particle diameter is another key factor in determining how nebulized aerosol medication behaves. Smaller particles can penetrate deeper into the respiratory tract, unlike larger particles, which tend to deposit in the upper airways.

Particulate matter

The term particulate matter includes characteristics of particle size distribution and particle diameter and evaluates them from a different point of view. It is a characterization of a mass of particles and summarizes the number of particles belonging into the smallest - ultra-fine particles, larger -fine particles, and coarse particles categories.

4.2.3 Nebulizer characterisation measurement

The first characterization measurement evaluates the performance of selected nebulizer devices. For representing the lungs a polymer bag with a volume of 2 liters is used.

To evaluate the performance of each nebulizer, the solution chamber of every device was filled with a 0.9% NaCl solution as specified by the respective manufacturer. Before, during, and post-measurement, the nebulizers were weighed to ascertain their output in milliliters and output rate in milliliters per minute. The simulator of breathing is turned on and stabilized for 30 seconds. Consequently, the spectrometer pump is turned on and stabilized for another 30 seconds. Finally, the nebulizer is turned on and measured for three minutes, three times in a row with re-weighting in between the measurements.

By measuring the number of particles (PN), particle number concentration (PNC) and particle size distribution by the optical aerosol spectrometer, the total aerosol output, and mass median diameter are determined at the end of nebulization. Using nebulization time, the aerosol output rate and percentage of fill volume emitted in 1 minute is calculated. After measurement a nebulizing system is re-weighted and the residual volume in the liquid chamber is determined.

4.2.4 Particle deposition measurement

Firstly, the liquid chamber in the nebulizer is filled with a volume predefined by their manufacturer. 30 seconds after turning on the breathing simulator, the spectrometer pumps are turned on and stabilized for another 30 seconds. Finally, the nebulizing system is turned on and operating for a nebulization time of 3 minutes.

At the end of nebulization, the nebulizer device is turned off first, and after that the simulator and pumps. The measurement is conducted 3 times for each to device to ensure accuracy and replicability. The change in particle size and total particle deposition in the mechanical Alberta model of upper airways and the porcine lungs within the respiratory system xPULM are determined. The exact steps taken to perform both measurements are listed in the appendices A and B.

5 Results

5.1 Evaluation of the measurement setup

5.1.1 Airtightness testing of manufactured components

Before conducting the actual measurement, a test for leakage of the setup was performed. The leakage from connectors was tested firstly by pressured gas and water bath when possible, and subsequently, in the complete setup by connecting it to a mechanical ventilator. In the CPAP mode and by using soap water, connections between components and the components themselves were tested for airtightness. Very small nanopores were proven to be present in the 3D printed connectors where the leaking air was creating bubbles. Sealing approaches like different printing parameters, high temperature post processing and using a sealant coating were considered. Starting from changing the temperature of the print and adding a number of walls into the print, the adjustment was succesfull and in further testing the connectors were proven to be airtight.

5.1.2 Breathing pattern adjustment

The setup was then tested by the xPULM breathing simulator using physiolgical breathing values of 15 breaths per minute, 0.5 l of tidal volume and 1:1 inhlation to exhalation ratio and incorporating flow sensors at the input and output. By measuring the flow in these two points it was discovered, that incorporated one-way valves are not working properly. In the image nb. 5.1 is shown an input and output flow in the measurement setup. In the parts marked by a star, the valve is suppose to be closed. In the output flow curve it is also possible to see an oscilation of the valve when trying to close.

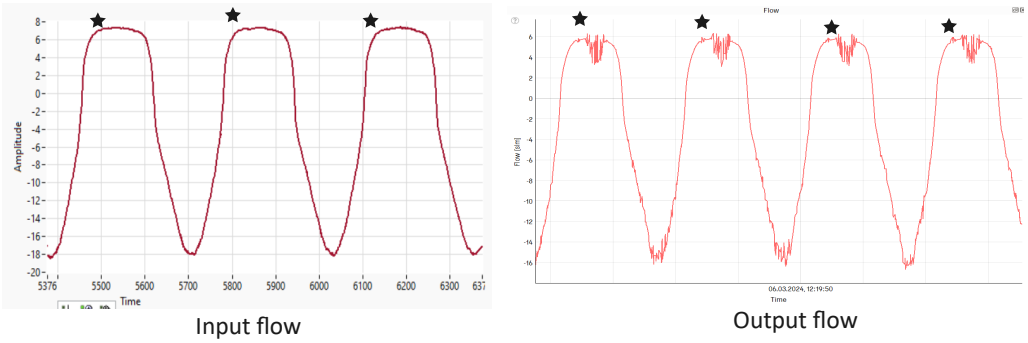

Fig. 5.1: Input and output flow in the measurement setup using original one-way valves.

A test on the valves Themselves was conducted using only a flow sensor and a mechanical ventilator. Different flow and pressure values were applied on the valves to see at which value they start to work correctly. As shown in the graph nb. 5.2 marked with stars, only after reaching a value of at least 2000 Pa (22 mbar), the valve started to close. This value is much higher than the value of pressure generated by physiological breathing, so the valve was concluded unusable. The membranes in the valves were replaced by thinner latex rubber bands that require lower values of flow and pressure to work which fixed this issue.

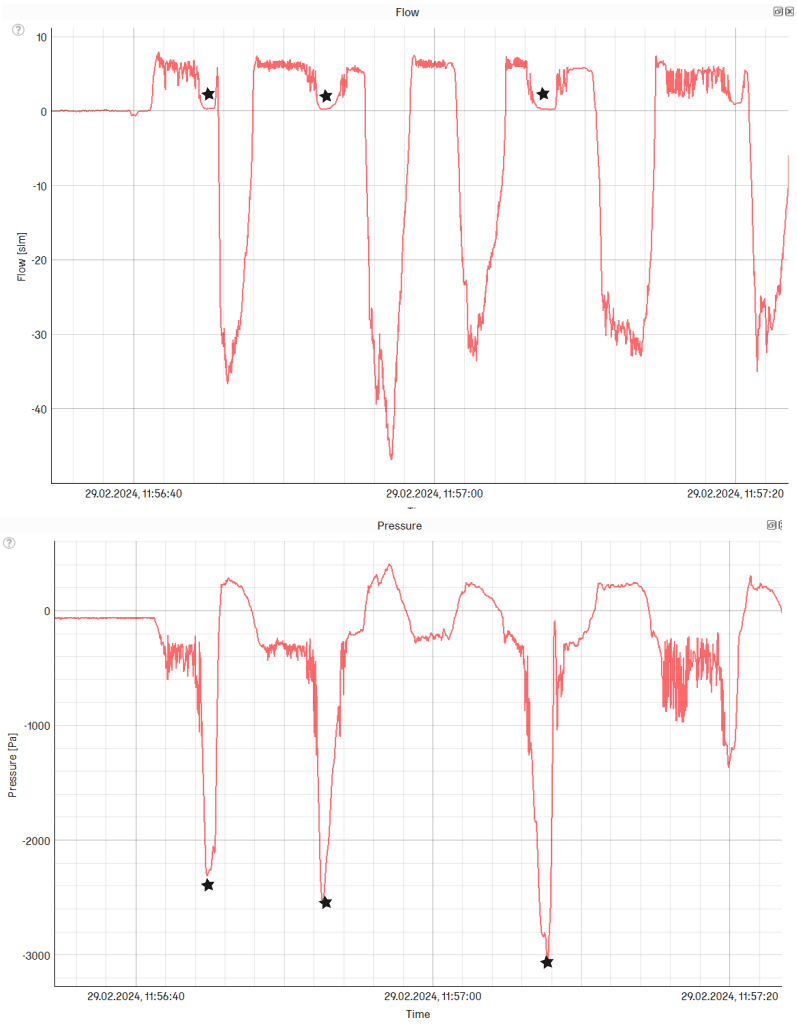

Fig. 5.2: Input and output flow of the measurement setup.

After exchanging the membranes in the valves, a difference of approximately 4 slm was present between the input and output flow values. The difference was assigned to the AUAM incorporated in the input pathway. Subsequently, the pressure drop generated by the AUAM was measured to determine the character of the models resistance for later corrective solution for the flow difference. By the results shown in the graph 5.3, the character of the resistence in the AUAM is polynomial,

confirmed by the value R of trend lines reliability that is almost 1. Due to this fact, a poynomial resistence was incorporated in the output pathway using a Pneuflow Resistor - Rp5, that is normally used in a Lung testing researches a simulator of physiological resistance in the airways [52, 53].

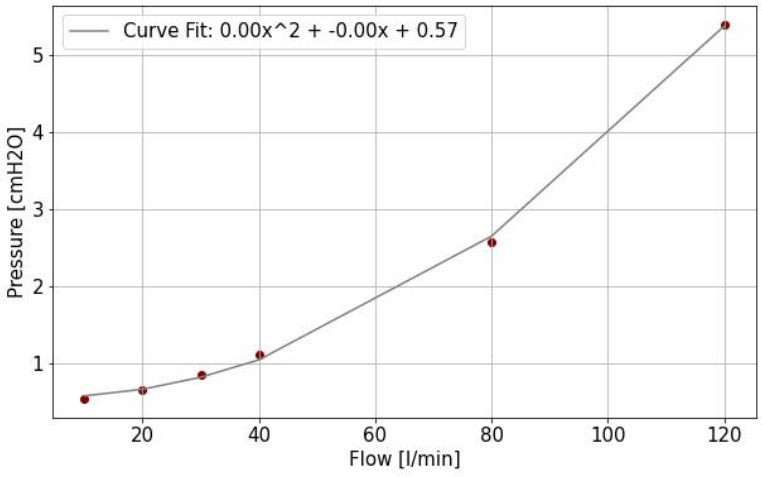

Fig. 5.3: The graph of relationship between flow in l/min and pressure drop in cmH_2O measured on the Alberat upper-airway model.

The graph 5.4 illustrates the effects of adjusting valves and introducing resistance on flow in the setup. Initially, the input flow stands at 22.5 slm, with a corresponding backflow of around 3 slm. The output flow is measured at 23 slm, similarly accompanied by a backflow of 3 slm. The final flow values reflect the intervention in improving flow dynamics within the system. By fine-tuning valves and incorporating resistance the flow characteristics were optimized.

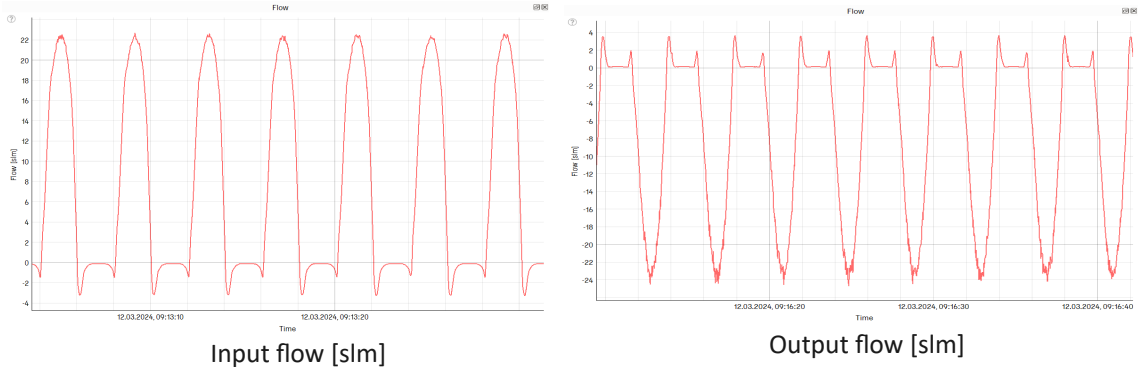

Fig. 5.4: Input and output flow of the measurement setup with corrected valves and incorporated resistence.

5.1.3 Tidal volume control

Another tested property of the setup was the input and output volume to confirm, that there is no leakage in the setup and the volume of inhaled and exhaled air while simulating breathing is the same. As the graph 5.5 shows, both the inhaled and exhaled volume are approximately 0.5 l, which is also a volume set by the xPULM for breathing simulations.

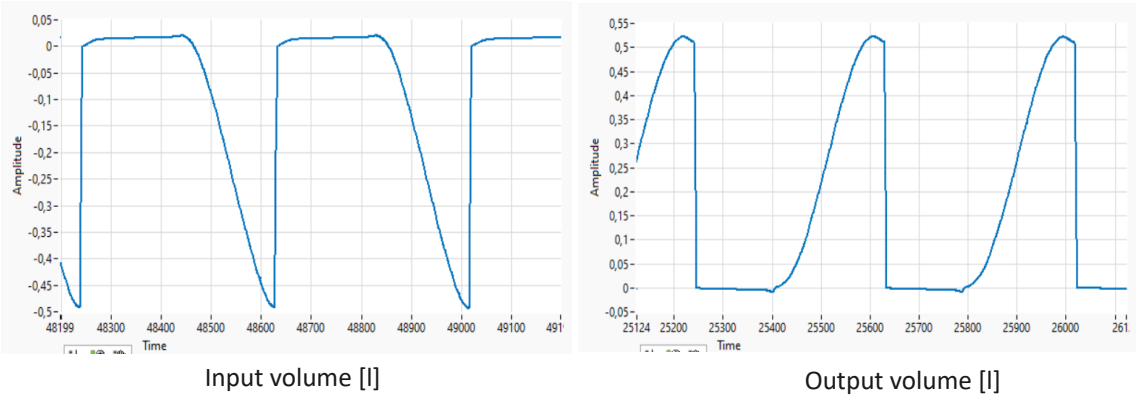

Fig. 5.5: Input and output values of volume wtih a input and output flow from graph 5.4.

5.1.4 Coincidence error

When conducting the test characterization measurements, a coincidence signal was observed. The coincidence signal or coincident error in optical spectrometers refers to a phenomenon, where two or more signals overlap and are not distinguishable from one another. This error can significantly impact the precision and accuracy of spectrometric measurements, affecting the reliability of the obtained data.

The wellas Sensor 2200 employed in this study possesses a size range spanning from 0.2 to 10 µm, with a particle number concentration limit of 16.000 P/cm^3. Initially, the nebulizers underwent multiple measurements without the use of a dilution chamber, revealing significantly concentrated solutions. Implementation of the dilution chamber effectively reduced the particle number concentration, minimizing the coincidence factor to the greatest extent possible.

In the figure 5.6 is shown, how the particle size distribution looks when the solution of 0.9% NaCl is measured in the low and the high coincidence state. Because of the absence of a shift in the size range and no significant differences in the mean particle diameter (for jet: 1.78 µm vs 1.45 µm, for ultrasonic: 3.72 µm vs. 3.78 µm and for mesh nebulizer: 2,49 µm vs. 1.76 µm), the final coincidences of 80% for jet nebulizer, 20% for ultrasonic nebulizer, and 80% for mesh nebulizer were accepted.

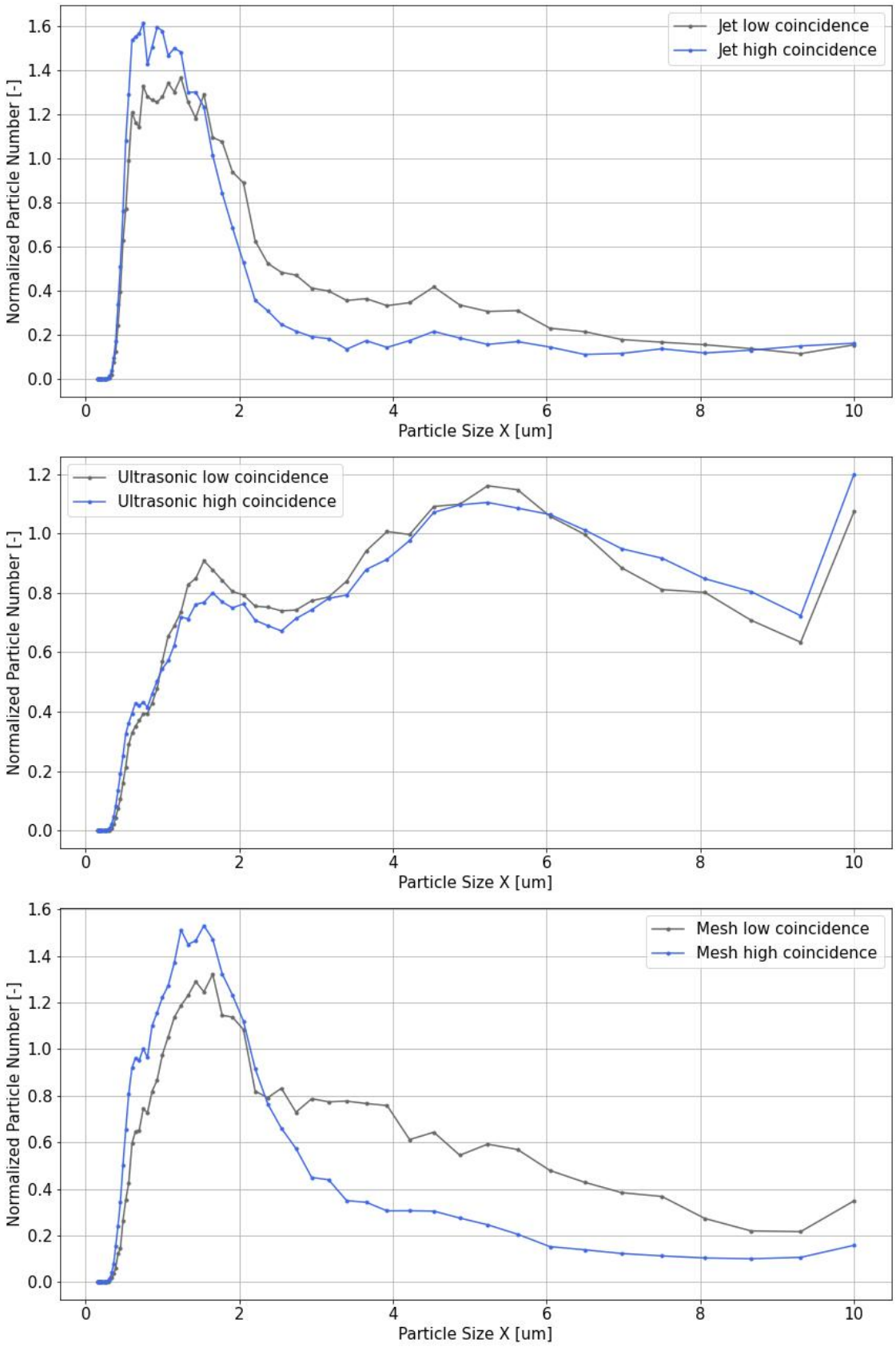

Fig. 5.6: Normalized particle number and particle size distribution measured with low and high coincidence signal by Palas Promo 2000 in combination with wellas sensor 2200 and A) jet nebulizer Medisana Inhalator IN 500 Compact, B) ultrasonic nebulizer Dittman Inhaler IHG 350 and C) mesh nebulizer Omron U100 Microair.

5.2 Nebulizer characterization measurement

All measurements were conducted under constant laboratory conditions adhering to 21 +/- 2 °C temperature, 45-75% humidity, and standard atmospheric pressure. The following table 5.1 summarizes the main characteristics obtained by this characterisation measurement aimed to evaluate the performance of tested devices.

Tab. 5.1: Characterisation measurement.

Nebulizer devices	Medisana Inhalator IN 500 Compact	Dittman Inhaler IHG 350	Omron U100 Microair
Measured Parameters			
Weight pre-measurement [g]	26	182	174
Weight post-measurement [g]	21	180	167
Liquid output [ml]	5	2	7
Residual Volume [ml]	5	6	1
Computed Parameters			
Aerosol Output [P]	388 579	496 414	688 803
Aerosol Output rate [P/min]	43 175	55 157	76 533
Output rate [ml/min]	0.55	0.22	0.77
Percentage of emitted volume[%]	50	25	87.5
Percentage of volume emitted per minute [%]	5.55	2.77	9.72
Mean particle diameter [µm]	1.52	3.9	1.78

5.2.1 Aerosol output and output rate

The pre-and post-measurement weights listed in the table were used for the computation of the nebulized milliliters of the aerosol. Among the observed measurements, the mesh nebulizer, Omron U100 MicroAir, exhibited the highest output, nearly fully nebulizing its 8-milliliter solution within the 9-minute duration. Conversely, the ultrasonic nebulizer, Dittman Inhaler IHG 350, demonstrated the lowest output, with only 2 milliliters nebulized. The jet nebulizer, Medisana Inhalator IN 500 Compact, consistently maintained a stable output of 5 milliliters in total.

Subsequent analysis of the results, conducted using Palas PDAnalyzer software, enabled estimation of aerosol output in particle number and aerosol output rate in particles per minute. Once again, the mesh Omron nebulizer exhibited the highest output and rate. Unlike the visual output, the jet nebulizer from Medisana displayed

the lowest aerosol output and output rate, with the ultrasonic Dittman nebulizer positioned between these two.

The entire nebulization process lasted 9 minutes and was divided into three 3-minute intervals from which values of particle output were averaged and listed in the table. Concurrently, the nebulizers were weighed during the process to monitor potential output fluctuations over time. Figure 5.7 illustrates the averaged aerosol outputs from the three intervals for all three nebulizer variants including the standard deviations. The biggest standard deviation in the aerosol output is present in the Mesh nebulizer and the smallest in the ultrasonic one.

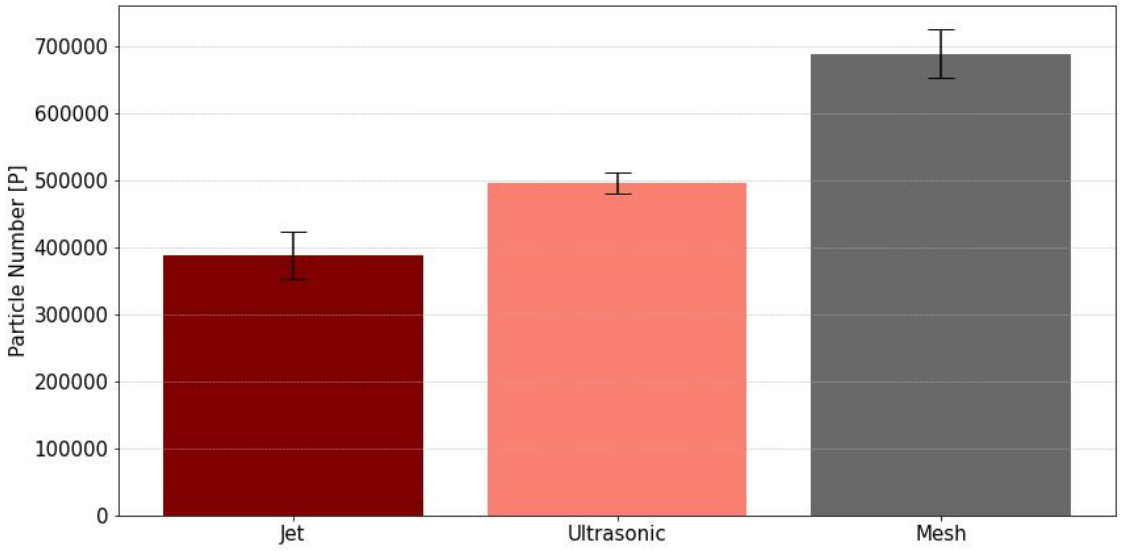

Fig. 5.7: Histogram of mean of Particle Number values with their standard deviations for 3 tested nebulizers: Jet Medisana Inhalator IN 500 Compact nebulizer, Ultrasonic Dittman Inhaler IHG 350 nebulizer and Mesh Omron U100 MicroAir nebulizer.

5.2.2 Residual volume

The Medisana jet nebulizer's fill volume was 10 milliliters, thus its 5-milliliter residual volume implies a 50% utilization rate, as illustrated in the figure 5.8. The ultrasonic Dittman and mesh Omron nebulizers were filled with 8 ml of testing solution, so 6 ml in the ultrasonic Dittman stand for 25%, and the 1 ml in the mesh Omron nebulizer displays highest efficiency of 87.5%. The percentage of volume emitted per minute was derived from the above percentage values and was 5.55% for the Medisana jet, 2.77% for ultrasonic Dittman, and 9.72% for Omron mesh nebulizer.

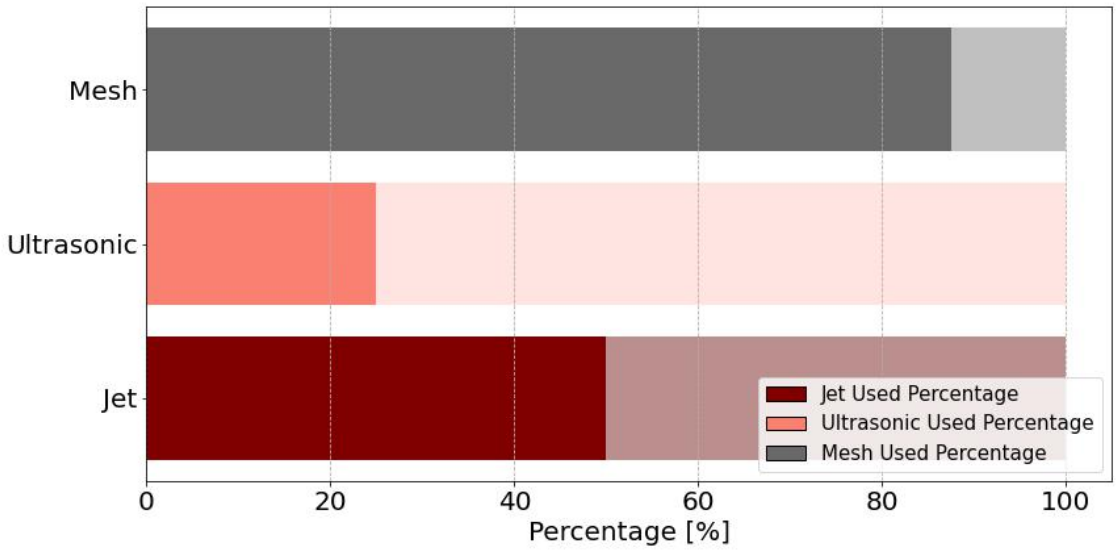

Fig. 5.8: Histogram displaying the percentage of used solution for the nebulization time of 9 minutes for 3 tested nebulizers: Jet Medisana Inhalator IN 500 Compact nebulizer, Ultrasonic Dittman Inhaler IHG 350 nebulizer and Mesh Omron U100 MicroAir nebulizer.

5.2.3 Particle size distribution

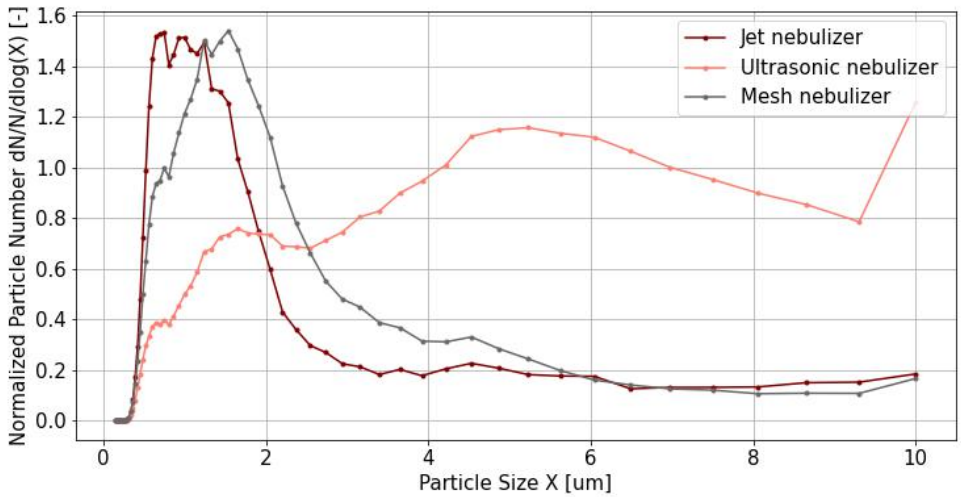

Fig. 5.9: Particle numbers and particle size distributions for 3 tested nebulizers: Jet Medisana Inhalator IN 500 Compact nebulizer, Ultrasonic Dittman Inhaler IHG 350 nebulizer and Mesh Omron U100 MicroAir nebulizer.

The resultant size distributions of nebulized particles displayed in relationship with particle number and particle number concentration are depicted in the figure 5.9. The Mesh Omron U100 MicroAir and Jet Medisana Inhalator IN 500 Compact nebulizers yielded the highest particle number and particle number concentration. Notably, their size distributions exhibited a relatively narrow profile, centered around a peak at 1.72 µm and 1.52 µm, representing their mean particle diameter.

Conversely, the size distribution for the Ultrasonic Dittman Inhaler IHG 350 nebulizer was notably broader, encompassing the entire spectrum of particles from 0.2 to 10 µm, with a peak observed at its mean particle diameter value of 3.90 µm.

5.2.4 Particle diameter

The measured mean optical particle diameters of nebulized aerosols and their standard deviations are illustrated in the boxplots in Figure 5.10, elucidating that the jet nebulizer produced the smallest particles, followed by the mesh nebulizer with slightly larger particles, and the ultrasonic nebulizer producing the largest particles.

The commonly referenced aerosol diameter is the aerodynamic diameter (MAD), while the diameter measured by OAS corresponds to the optical aerosol diameter. An equation 2.1 for conversion was employed. The computed aerodynamic equivalents marginally exceed the measured optical diameters. Specifically, the MAD for jet nebulizers is calculated as 2.05 µm, for ultrasonic nebulizers as 4.52 µm, and for mesh nebulizers as 2.26 µm.

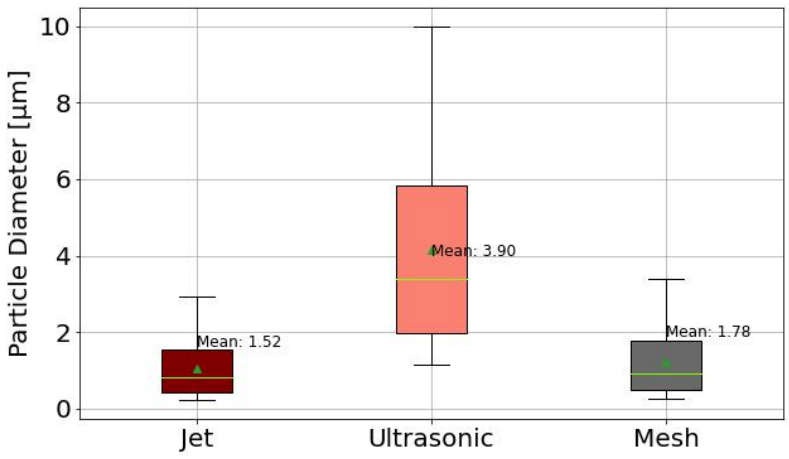

Fig. 5.10: Boxplot of measured optical partical diameters for 3 tested nebulizers: Jet Medisana Inhalator IN 500 Compact nebulizer, Ultrasonic Dittman Inhaler IHG 350 nebulizer and Mesh Omron U100 MicroAir nebulizer.

5.2.5 Particulate matter

Table 5.2 presents the percentages of particulate matter smaller than 1 µm and 2.5 µm out of the total particulate matter. These values confirm the previously discussed size distribution results. For instance, the jet Medisana nebulizer, with a mean particle diameter of 1.52 µm, primarily generated particles smaller than 2.5 µm but not smaller than 1 µm.

The ultrasonic Dittman nebulizer, with a mean particle diameter of 3.90 µm, produced a very limited quantity of particles smaller than 1 µm, with less than half falling below 2.5 µm. The majority of particles then fall in the range from 2.5 to 10 µm.

The mesh Omron nebulizer, similar to the jet Medisana nebulizer, has a high quantity of small particles. With the mean particle diameter of 1.72 µm, approximately one-third of the particles have a smaller diameter than 1 µm, while the majority fall below 2.5 µm.

Tab. 5.2: Percentage of produced particulate matter.

Nebulizer type	Jet Medisana Inhalator	Ultrasonic Dittman Inhaler	Mesh Omron Microair
PM1 [%]	23.45	14.47	33.86
PM2.5 [%]	62.72	42.47	84.58

5.3 Aerosol deposition measurement

The objective of this aerosol measurement was to discern the deposition patterns of particles within various segments of the simulated respiratory tract. The results obtained from the three sampling points provide insight into the particle size distribution and characteristics, including particle number, particle number concentration, and particulate matter composition, observed before entry into the respiratory tract representation, subsequent passage through the upper airway Alberta model, and at the exit from the porcine lungs.

5.3.1 Particle size distribution comparison

As the nebulized aerosol traverses the respiratory tract and undergoes particle deposition, alterations in the aerosol's size distribution can occur. Figure 5.11 A), B), and C) illustrate the relationships between particle size distributions and the corresponding particle number and concentration values of the aerosol produced by the evaluated nebulizers at all three sampling points.

Consistent with previous characterization measurements, the input size distribution maintains its shape, with the narrowest distribution observed from the jet Medisana nebulizer and the widest from the ultrasonic Dittman nebulizer. Mesh Omron generated the highest PN and PNC values, followed closely by the jet Medisana, with the ultrasonic Dittman trailing behind.

The size distribution of aerosols after passing through the AUAM showed minimal change across all three representations. The most pronounced decrease in PN and PNC is present in the figure 5.11 B). The wide distribution indicates particles with larger diameters that have a tendency to deposit more in the upper airways. Despite the observed decrease, the distribution does not undergo significant shifting.

A more substantial shift in the distributions is present in the curves illustrating the distribution of aerosol particles after passing through the porcine lungs. These distributions are narrower and predominantly concentrated around smaller diameters, approximately 1.5 to 2 µm. The majority of particles larger than this diameter were deposited within the representation of the respiratory tract.

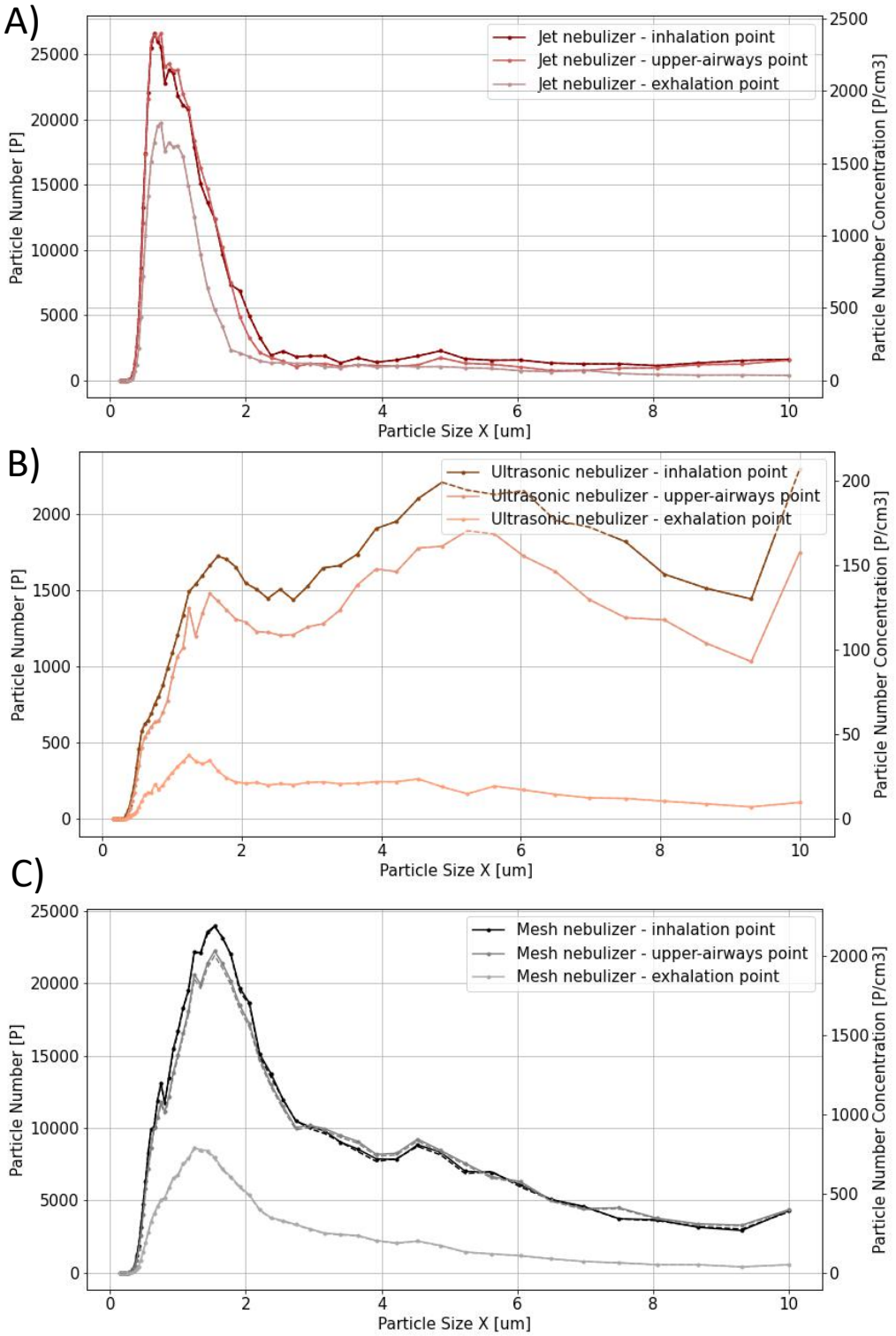

Fig. 5.11: Particle number and particle number concentration displayed with size distribution for 3 tested nebulizers: A) Jet Medisana Inhalator IN 500 Compact nebulizer, B) Ultrasonic Dittman Inhaler IHG 350 nebulizer and C) Mesh Omron U100 MicroAir nebulizer for 3 sampling points: before entering the upper airway Alberat model, after passing through upper airway Alberta model and after the one-way valve at the output.

5.3.2 Change in the particle diameter

As particles undergo deposition, the measured mean particle diameter of the particles changes. Across all three boxplots in 5.12 a slight reduction in particle diameter is observable. As the bigger particles deposit sooner in the respiratory tract, only smaller ones pass through the upper airways and only the smallest through the porcine lungs.

The Jet Medisana Inhalator IN 500 Compact nebulizer, already producing very small particles, changed from 1.26 µm to 1.18 µm after passing through the AUAM and to 1.13 µm after passing through the porcine lungs.

The most substantial shift occurred in the aerosol with the originally highest mean particle diameter of 3.79 µm generated by the Ultrasonic Dittman Inhaler IHG 350 nebulizer, which reduced to 3.71 µm after passing through AUAM and to 2.69 µm after passing through the porcine lungs.

Interestingly, in the aerosol generated by the Mesh Omron U100 MicroAir nebulizer, the mean particle diameter exhibited a slight increase after traversing the AUAM, from 2.23 to 2.33 µm. However, upon passage through the porcine lungs, it eventually decreased to 1.88 µm.

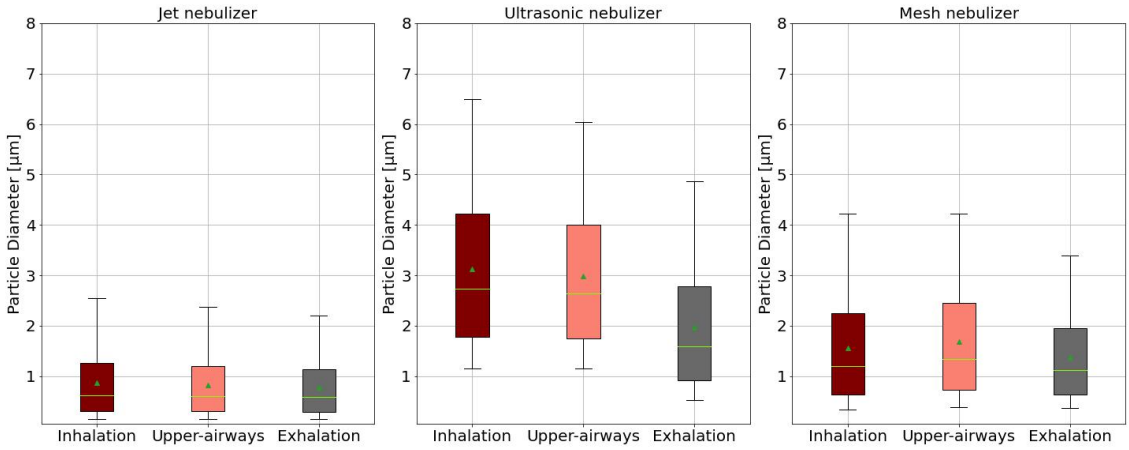

Fig. 5.12: Boxplot of measured optical partical diameters for 3 tested nebulizers: Jet Medisana Inhalator IN 500 Compact nebulizer, Ultrasonic Dittman Inhaler IHG 350 nebulizer and Mesh Omron U100 MicroAir nebulizer for 3 sampling points: before entering the upper airway Alberat model, after passing through upper airway Alberta model and after the one-way valve at the output.

5.3.3 Change in the particulate matter

Examining the percentage of particulate matter provides another perspective on characterizing the nebulized aerosol. Particles depositing in the final parts of the respiratory tract, in the alveolar region, have the smallest diameters, so the bigger the percentage in the PM1 and PM2.5 categories, the higher the chances for deposition in these final regions.

The highest percentages, as depicted in the table 5.3 belong to the Jet Medisana Inhalator IN 500 Compact nebulizer with almost all of the particles smaller than 2.5 µm. Given the minimal alterations observed in size distribution and particle diameters of the aerosol generated by this nebulizer, the PM values at various sampling points remain quite similar. The escalating values at these points suggest an increased representation of particles with smaller mean diameters.

Conversely, the Ultrasonic Dittman Inhaler IHG 350 nebulizer showcased the most pronounced alterations in particle size distributions, mean diameters, and particulate matter percentages. The PM1 values increased by almost 8% and the PM2.5 values even by almost 20%. It completes the previously presented data of the high deposition of particles generated by this nebulizer.

The changes in the aerosol generated by the Mesh Omron U100 MicroAir nebulizer were more notable than those from the jet nebulizer but less pronounced than those from the ultrasonic variant. The increases were primarily observed in the PM2.5 category, rising by approximately 5%.

Tab. 5.3: Change in the produced particulate matter due to sampling points.

Sampling point	PM1 [%]	PM2.5 [%]
Jet nebulizer inhalation point	61.48	93.1
Jet nebulizer upper-airways point	63.14	94.94
Jet nebulizer exhalation point	66	94.42
Ultrasonic nebulizer inhalation point	13.24	44.61
Ultrasonic nebulizer upper-airways point	13.22	45.18
Ultrasonic nebulizer exhalation point	21.44	63.14
Mesh nebulizer inhalation point	25.19	74.91
Mesh nebulizer upper-airways point	24.05	70.33
Mesh nebulizer exhalation point	25.75	81.39

5.3.4 Deposition in the respiratory tract

In the figures 5.13 and 5.14 are shown the percentages of deposited aerosol particles after passing through the Alberta upper-airway model and after passing through either porcine lungs or polymer bag.

Deposition in upper-airways

In both scenarios, whether utilizing polymer or porcine lungs, deposition in the upper airways is small. The smallest deposition, 8.76% and 1.46%, in the upper airways occurred with aerosols generated by the Jet Medisana Inhalator IN 500 Compact nebulizer. Slightly higher, 11.23% and 5.28%, in aerosol from the Mesh Omron U100 MicroAir nebulizer and the highest, 12.8% and 17.87%, in the aerosol nebulized by the Ultrasonic Dittman Inhaler IHG 350 nebulizer. The values differ when using polymer bags and porcine lungs.

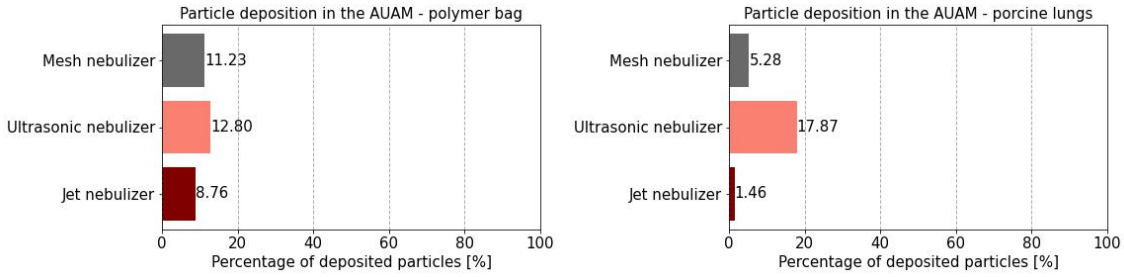

Fig. 5.13: Histogram of calculated particle deposition in different parts of the representation of upper airways for 3 tested nebulizers: Jet Medisana Inhalator IN 500 Compact nebulizer, Ultrasonic Dittman Inhaler IHG 350 nebulizer and Mesh Omron U100 MicroAir nebulizer.

Deposition in the porcine lung and polymer bag

The deposition of particles in the porcine lungs was visibly greater than in the polymer bag. The Mesh Omron U100 MicroAir nebulizer deposited with a percentage of 67.4% in the porcine lungs against 53.1% in the polymer bag. The difference between deposition values in these two variants was the smallest.

84.8% of particles generated by the Ultrasonic Dittman Inhaler IHG 350 deposited in the porcine lungs while only 12.89% deposited in the polymer bag. The percentage of particles generated by this ultrasonic nebulizer and deposited in the porcine lungs was the greatest.

The particles from the Jet Medisana Inhalator IN 500 Compact had smallest values of percentage of particle deposition. Only 33.98% of particles deposited in the porcine lungs and 18.55% of particles deposited in the polymer bag. The difference between these two values is also not very significant.

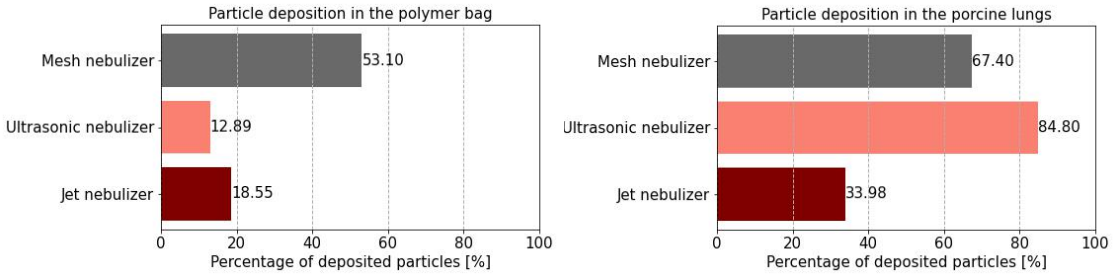

Fig. 5.14: Histogram of calculated particle deposition in different parts of the representation of upper airways for 3 tested nebulizers: Jet Medisana Inhalator IN 500 Compact nebulizer, Ultrasonic Dittman Inhaler IHG 350 nebulizer and Mesh Omron U100 MicroAir nebulizer.

6 Discussion

6.1 Setup design

After thorough research in nebulizing system testings and nebulized aerosol measurements, a first experimental setup was designed. The components like the Alberta model as the upper-airway structure, and porcine lungs and polymer bags as human lung equivalents within the xPULM breathing simulator were selected to represent the human respiratory tract. Additional components enabling measurement control like flow sensors and one-way valves were incorporated into the setup using 3D modeled and printed connections. The dilution chamber and resistance simulator were other supplementary components built in after conducting the first testing measurements. Optical aerosol spectroscopy allowed for measurement to be conducted multiple times in a row and to be observed in real time.

6.2 Setup assembly

After assembling everything together, the results from the setup testing phase provided crucial insights into the functionality and reliability of the experimental apparatus used in the subsequent characterization and deposition measurements. Four key aspects were evaluated: material leakage, flow adjustment, volume control, and coincidence error.

Before conducting the actual measurements, it was essential to ensure the airtightness of the setup to prevent any unintended that could compromise the accuracy of the results. Testing revealed small nanopores in the 3D-printed connectors, leading to air leakage. Various sealing approaches were explored, including sealant coating, heat treatment, and print settings adjustment. Ultimately, successful adjustments were made, ensuring the airtightness of the connectors.

To secure the same flow in both, the inhalation and exhalation pathways in the setup, and to further optimize flow characteristics, the resistance in the output pathway was incorporated. The evaluation of flow dynamics within the setup revealed issues with the original one-way valves, condemning them unsuitable for physiological breathing simulations. Replacement of the valve membranes with thinner latex rubber bands improved this issue. Anyway, after conducting all of the measurements, this adjustment was not sufficient enough. A backflow of 3 - 6 l/min was present in both valves, causing some inaccuracies in the measured aerosol data. In the future, perfectly one-way valves should be used for this measurement purpose.

Ensuring consistent input and output volumes was critical for accurate simulation of respiratory conditions. Testing confirmed, that after adjusting the flow in

both pathways, both inhaled and exhaled volumes were approximately 0.5 liters, aligning with the physiological parameters set by the breathing simulator.

The observation of coincidence signals in optical spectrometers, can introduce significant errors in measurements, impacting data precision and reliability. High coincidence signals were initially observed, necessitating the incorporation of a dilution chamber into the setup. Subsequent analysis revealed acceptable levels of coincidence for each nebulizer variant, ensuring the accuracy of the characterization measurements.

6.3 Nebulizer evaluation measurement

The nebulizer characterization measurement conducted in this study provided valuable insights into the performance and efficiency of three different nebulizer devices: the Medisana Inhalator IN 500 Compact, Dittman Inhaler IHG 350, and Omron U100 MicroAir. A comprehensive analysis of various parameters including aerosol output, output rate, residual volume, particle diameter, and size distribution was presented.

6.3.1 Aerosol output and output rate evaluation

Tab. 6.1: Comparison of aerosol output rate given by a manufacturer and measured in the thesis.

Nebulizer type	Aerosol output rate [ml/min] - manufacturer	Aerosol output rate [ml/min] - measured
Medisana Inhalator IN 500 Compact	0.2	0.55
Dittman Inhaler IHG 350	0.25	0.22
Omron U100 Microair	0.1	0.77

The measured aerosol output and output rates offered a quantitative assessment of each nebulizer's performance in delivering medication. Notably, the mesh nebulizer, Omron U100 MicroAir, demonstrated superior performance with the highest aerosol output and output rate in milliliters and particle numbers. This finding aligns with previous research highlighting the efficiency of mesh nebulizers in generating fine aerosol particles suitable for deep lung deposition.

In particle numbers, the jet Medisana Inhalator IN 500 Compact, exhibits the lowest aerosol output and aerosol output rate, although the output in milliliters is higher than ultrasonic Dittman Inhaler IHG 350. It shows that both of them have some limitations in their ability to efficiently nebulize medication.

When comparing the aerosol output rate given by the nebulizer manufacturer, the output rate in milliliters differs. The output rate given by the manufacturer in the table 6.3.1 is the minimal value that the nebulizer is supposed to give and those values were met.

6.3.2 Residual volume evaluation

The evaluation of residual volume provided crucial insights into the efficiency of each nebulizer in delivering the intended dose of medication. A lower residual volume indicated higher efficiency in medication delivery, as more of the solution is effectively nebulized. In this study, the mesh nebulizer, Omron U100 MicroAir, stood out with the lowest residual volume and highest efficiency of 87.5%. This implies that the Omron nebulizer can deliver a greater proportion of the medication to the patient compared to the other tested devices.

Conversely, the ultrasonic nebulizer, Dittman Inhaler IHG 350, exhibited the highest residual volume and lowest efficiency among the tested devices. Medisana Inhalator IN 500 Compact successfully used only 50% of its capacity. These findings highlight the importance of optimizing nebulizer design and technology to maximize medication delivery efficiency and minimize waste.

6.3.3 Particle size distribution and diameter evaluation

The size distribution of aerosol particles plays a critical role in determining their deposition patterns within the respiratory tract and ultimately, their therapeutic efficiency. The analysis of particle diameter and size distribution revealed notable differences among the tested nebulizers.

The mesh nebulizer, Omron U100 MicroAir, and jet nebulizer, Medisana Inhalator IN 500 Compact consistently produced aerosol particles with a relatively narrow size distribution and a mean particle diameter conducive to deep lung deposition. In contrast, the ultrasonic nebulizer, Dittman Inhaler IHG 350, generated aerosol particles with a broader size distribution and larger mean particle diameter, potentially limiting their penetration into the lower airways.

When comparing measured mean particle diameters with the ones given by the manufacturer in the table 6.2, their values fall within the given range but especially in jet and mesh nebulizers are smaller than anticipated.

Tab. 6.2: Comparison of particle diameter given by a manufacturer and measured in the thesis.

Nebulizer type	Particle diameter [µm] - manufacturer	Particle diameter [µm] - measured
Medisana Inhalator IN 500 Compact	<5	2.05
Dittman Inhaler IHG 350	<5	4.52
Omron U100 Microair	<4.5	2.26

6.4 Aerosol deposition measurement

By analyzing the data collected from three distinct sampling points, interesting insights into the distribution and characteristics of particles were obtained. These observations were made before entry into the simulated respiratory tract, upon passage through the upper airway model Alberta, and upon exiting the porcine lungs or polymer bag.

6.4.1 Shift in the particle size distribution

The first analyzed matter was the shift in the size distribution of aerosol particles as they traveled through the respiratory tract. Graphical representations illustrated the relationships between particle size distributions and corresponding particle number and concentration values at each sampling point. Analysis revealed minimal changes in the size distributions of aerosols after passing through the AUAM in the Jet Medisana Inhalator IN 500 Compact and Mesh Omron U100 MicroAir nebulizers with generally small mean particle diameters. Larger particles, on the other hand, tend to deposit in the upper airways, which was partly confirmed by slightly narrower distribution and higher deposition in the curve of the Ultrasonic Dittman Inhaler IHG 350 nebulizer.

However, upon passage through the porcine lungs, significant shifts in particle distributions were observed, with narrower distributions centered around smaller diameters. This trend suggested a more substantial deposition of larger particles within the simulated respiratory tract.

6.4.2 Change of the particle diameter

Another analysis dealt with alterations in the mean particle diameter across all nebulizers. Rather small but consistent reductions were observed, indicating that the larger particles deposit sooner in the respiratory tract. Notably, the Ultrasonic Dittman nebulizer exhibited the most substantial reduction in mean particle diameter, probably due to the biggest mean diameter out of all tested devices.

Analysis of particulate matter percentages provided further insight into aerosol deposition, with higher percentages indicating increased deposition potential in the final regions of the respiratory tract. Disparities between nebulizer types were evident with the Jet Medisana nebulizer demonstrating minimal alterations in particulate matter percentages, while the Ultrasonic Dittman nebulizer exhibited pronounced shifts, underlining its probability for higher particle deposition.

6.4.3 Comparison of deposition in the porcine lungs and polymer bag

Finally, a comparison of deposition in porcine lungs versus polymer bags highlighted the superior suitability of porcine lungs for mimicking human lung behavior. Substantial differences in deposition underscored the limitations of polymer bag simulations in replicating real lung processes, emphasizing the importance of utilizing more physiologically representative models in aerosol deposition studies.

It is clearly visible, in the graphs 5.13 and 5.14, that the percentage values were not ideal. The first disparity is seen in the different deposition in the Alberta upper-airway model when using porcine lungs and polymer bag. The percentage of particle deposition in the AUAM is markedly higher when measured by utilizing the polymer bag. It is probably due to the lower particle deposition insight the polymer bag, that caused more concentrated aerosol exiting the representation and because of the inefficiency of one-way valves, some amount of the more concentrated aerosol entered the sampling point measuring the deposition of aerosol in the AUAM.

The higher deposition in the porcine lungs resolved in the less concentrated aerosol exiting the representation, so fewer aerosol particles flew with the backflow into the sampling point measuring the aerosol deposition in the AUAM.

The deposition in the porcine lungs is as anticipated much higher than in the polymer bag. Nevertheless, it is still lower than expected due to the other aerosol deposition studies. The deposition in the polymer bag is on the other hand higher than anticipated. These inaccuracies are also attributed to the dysfunction of one-way valves not being able to accurately and efficiently separate the inhaled and exhaled aerosol.

Conclusion

The presented study dealt with the experimental evaluation of different types of medical nebulizers that were examined from numerous aspects. At the beginning of the thesis, the main anatomical parts of the respiratory tract along with the main physiological parameters relevant to the assessment of breathing were presented along with the most common pathophysiological states, commonly treated by inhalation therapy.

Medical aerosols and methods of their production were also elucidated in the introduction part of the thesis. Medical nebulizers, as one of the approaches of the generation of aerosols, were explained in detail. The basic properties of aerosol particles like size, shape, or particle diameter, and principles of behavior leading to aerosol deposition by different mechanisms in the respiratory tract were also explained.

In the practical part of the thesis, an experimental setup was designed and assembled from selected components uniting nebulizer system testing standards and other experimental studies. Preceding the official measurements, a series of preliminary tests was conducted. Issues such as material leakage, flow dynamics, volume control, and coincidence error were addressed to enhance the validity of the data obtained during the following measurements.

The characterization measurement of the tested nebulizer devices provided comprehensive insights into their performance metrics and their potential for deposition in different parts of the respiratory tract. The deposition measurement underlined the importance of the correct choice of the device for inhalation therapy to access the target areas in the respiratory tract.

Overall, the design and assembly of the experimental setup brought new inquiries on the factors influencing the nebulizer evaluation process. It showed it is important to choose the correct testing solution and to combine it with the right measurement technique, taking into account the solutions concentration. The connections between utilized components and the connectors themselves need to be airtight to prevent any losses of measured aerosol particles. Proper separation of inhaled and exhaled air was found to be the most troubled and essential factor securing the accuracy of the measurement.

Future research could focus on improving these weak spots and continue with evaluating the nebulizers by simulating pathological breathing patterns typical for the pathologies that are most commonly treated by these devices.

Bibliography

[1] MINTZ, Matthew L., 2006. *Disorders of the respiratory tract: common challenges in primary care*. Totowa USA: Humana Press. ISBN: 978-1-58829-556-9.

[2] PATWA, Apeksh and SHAH, Amit, 2015. Anatomy and physiology of respiratory system relevant to anaesthesia. Online. *Indian Journal of Anaesthesia*. Roč. 59, č. 9. Available at: `https://doi.org/10.4103/0019-5049.165849`.

[3] DAVIES, Andrew and MOORES, Carl, 2010. STRUCTURE OF THE RESPIRATORY SYSTEM, RELATED TO FUNCTION. Online. In: *The Respiratory System*. Elsevier, p. 11-28. Available at: `https://doi.org/10.1016/B978-0-7020-3370-4.00002-5`.

[4] DIJEMENI, Esuabom, 2018. *Design and Development of Drug-Induced Sleep Endoscopy Classification System, Data Fusion System and Relational Data Model*. Dissertation. London: Imperial College London.

[5] DOWNEY, Ryan P. a Navdeep S. SAMRA, 2023. Anatomy, Thorax, Tracheobronchial Tree. *StatsPearls*. 4.

[6] AMADOR, Christina, Carly WEBER a Matthew VARACALLO, 2023. Anatomy, Thorax, Bronchial. *StatsPearls*. 6.

[7] SEADLER, Benjamin D., Fadi TORO a Sandeep SHARMA, 2023. Physiology, Alveolar Tension. *StatsPearls*. 3.

[8] *Airway and Alveolar Anatomy*, 2021. Online. Life in the fast line. Available at: `https://partone.litfl.com/airway_and_alveolar_anatomy.html#id`.

[9] PRICE, Dominique N.; KUNDA, Nitesh K. and MUTTIL, Pavan, 2019. Challenges Associated with the Pulmonary Delivery of Therapeutic Dry Powders for Preclinical Testing. Online. *KONA Powder and Particle Journal*. Roč. 36, s. 129-144. Available at: `https://doi.org/10.14356/kona.2019008`.

[10] BERNACIKOVÁ, Martina, 2012. *Physiology*. Brno: Masaryk University. ISBN 978-80-210-5840-2.

[11] WIKIPEDIA. *Lung Volumes*. Online. Available at: `https://en.wikipedia.org/wiki/Lung_volumes`.

[12] KUDO, Makoto; ISHIGATSUBO, Yoshiaki and AOKI, Ichiro. Pathology of asthma. Online. *Frontiers in Biology*. Roč. 2013, s. 16. Available at: `https://doi.org/10.3389/fmicb.2013.00263`.

[13] MACNEE, William, 2003. COPD: causes and pathology. Online. *Medicine*. Roč. 31, č. 12, s. 71-75. Available at: https://doi.org/10.1383/medc.31.12.71.27170.

[14] SHEPPARD, M.N. and NICHOLSON, A.G., 2002. The pathology of cystic fibrosis. Online. *Current Diagnostic Pathology*. Roč. 8, č. 1, s. 50-59. Available at: https://doi.org/10.1054/cdip.2001.0088.

[15] Expert consensus on nebulization therapy in pre-hospital and in-hospital emergency care, 2019. Online. *Annals of Translational Medicine*. Roč. 7, č. 18, s. 487-487. Available at: https://doi.org/10.21037/atm.2019.09.44.

[16] ARNOTT, Andrew; WATSON, Malcolm and SIM, Malcolm. Nebuliser therapy in critical care: The past, present and future. Online. *Journal of the Intensive Care Society*. Available at: https://doi.org/10.1177/17511437231199899.

[17] VALLORZ, Ernest; SHETH, Poonam and MYRDAL, Paul, 2019. Pressurized Metered Dose Inhaler Technology: Manufacturing. Online. *AAPS PharmSciTech*. Roč. 20, č. 5. Available at: https://doi.org/10.1208/s12249-019-1389-9.

[18] KOMALLA, Varsha; WONG, Chun Yuen Jerry; SIBUM, Imco; MUELLINGER, Bernhard; NIJDAM, Wietze et al., 2023. Advances in soft mist inhalers. Online. *Expert Opinion on Drug Delivery*. 2023-08-03, roč. 20, č. 8, s. 1055-1070. Available at: https://doi.org/10.1080/17425247.2023.2231850.

[19] DAL NEGRO, Roberto W, 2015. Dry powder inhalers and the right things to remember: a concept review. Online. *Multidisciplinary Respiratory Medicine*. Roč. 10, č. 1. Available at: https://doi.org/10.1186/s40248-015-0012-5.

[20] ARI, Arzu, 2014. Jet, Ultrasonic, and Mesh Nebulizers: An Evaluation of Nebulizers for Better Clinical Outcomes. Online. *Eurasian Journal of Pulmonology*. 2014-5-12, roč. 16, č. 1, s. 1-7. Available at: https://doi.org/10.5152/ejp.2014.00087.

[21] ELPHICK, Mark; VON HOLLEN, Dirk; PRITCHARD, John N; NIKANDER, Kurt; HARDAKER, Lucy EA et al., 2015. Factors to consider when selecting a nebulizer for a new inhaled drug product development program. Online. *Expert Opinion on Drug Delivery*. 2015-06-17, roč. 12, č. 8, s. 1375-1387. Available at: https://doi.org/10.1517/17425247.2015.1014339.

[22] TAYLOR, Kevin M.G and MCCALLION, Orla N.M, 1997. Ultrasonic nebulisers for pulmonary drug delivery. Online. *International Journal of Pharmaceutics*. Roč. 153, č. 1, s. 93-104. Available at: https://doi.org/10.1016/S0378-5173(97)00105-1.

[23] PEDERSEN, Kenneth Manby; HANDLOS, Vagn Neerup; HESLET, Lars and KRISTENSEN, Henning Gjelstrup, 2006. Factors Influencing the In Vitro Deposition of Tobramycin Aerosol: A Comparison of an Ultrasonic Nebulizer and a High-Frequency Vibrating Mesh Nebulizer. Online. *Journal of Aerosol Medicine*. Roč. 19, č. 2, s. 175-183. Available at: https://doi.org/10.1089/jam.2006.19.175.

[24] VECELLIO, Laurent; DE GERSEM, Ruth; LE GUELLEC, Sandrine; REYCHLER, Gregory; PITANCE, Laurent et al., 2011. Deposition of aerosols delivered by nasal route with jet and mesh nebulizers. Online. *International Journal of Pharmaceutics*. Roč. 407, č. 1-2, s. 87-94. Available at: https://doi.org/10.1016/j.ijpharm.2011.01.024.

[25] AGRANOVSKI, Igor, 2010. *Aerosols: science and technology*. Weinheim: Wiley-VCH Verlag GmbH & Co. ISBN 978-3-527-32660-0.

[26] NATIONAL SCIENCE FOUNDATION CENTER FOR CHEMICAL INNOVATION, 2020. Introduction to Aerosols. *CAICE* [online]. [cit. 2024-01-07]. Available at: https://caice.ucsd.edu/introduction-to-aerosols/

[27] A basic guide to particle characterization, 2015. *Malvern Instruments Worldwide*. S. 24.

[28] CHIEN, Chih-Hsiang; THEODORE, Alexandros; WU, Chang-Yu; HSU, Yu-Mei and BIRKY, Brian, 2016. Upon correlating diameters measured by optical particle counters and aerodynamic particle sizers. Online. *Journal of Aerosol Science*. Roč. 101, s. 77-85. Available at: https://doi.org/10.1016/j.jaerosci.2016.05.011.

[29] DARQUENNE, Chantal, 2012. Aerosol Deposition in Health and Disease. Online. *Journal of Aerosol Medicine and Pulmonary Drug Delivery*. Roč. 25, č. 3, s. 140-147. Available at: https://doi.org/10.1089/jamp.2011.0916.

[30] LÖNDAHL, Jakob; MÖLLER, Winfried; PAGELS, Joakim H.; KREYLING, Wolfgang G.; SWIETLICKI, Erik et al., 2014. Measurement Techniques for Respiratory Tract Deposition of Airborne Nanoparticles: A Critical Review. Online. *Journal of Aerosol Medicine and Pulmonary Drug Delivery*. Roč. 27, č. 4, s. 229-254. Available at: https://doi.org/10.1089/jamp.2013.1044.

[31] LEPISTÖ, Teemu; KUULUVAINEN, Heino; JUUTI, Paxton; JÄRVINEN, Anssi; ARFFMAN, Anssi et al., 2020. Measurement of the human respiratory tract deposited surface area of particles with an electrical low pressure impactor. Online. *Aerosol Science and Technology*. 2020-08-02, roč. 54, č. 8, s. 958-971. Available at: `https://doi.org/10.1080/02786826.2020.1745141`.

[32] THE UNIVERSITY OF MANCHESTER. Scanning Mobility Particle Sizer. *Centre for Atmospheric Science* [online]. [cit. 2024-01-07]. Available at: `http://www.cas.manchester.ac.uk/restools/instruments/aerosol/scanning/`

[33] LOWTHER, Scott D.; JONES, Kevin C.; WANG, Xinming; WHYATT, J. Duncan; WILD, Oliver et al., 2019. Particulate Matter Measurement Indoors: A Review of Metrics, Sensors, Needs, and Applications. Online. *Environmental Science & Technology*. 2019-10-15, roč. 53, č. 20, s. 11644-11656. Available at: `https://doi.org/10.1021/acs.est.9b03425`.

[34] KOULLAPIS, P.; KASSINOS, S.C.; MUELA, J.; PEREZ-SEGARRA, C.; RIGOLA, J. et al., 2018. Regional aerosol deposition in the human airways: The SimInhale benchmark case and a critical assessment of in silico methods. Online. *European Journal of Pharmaceutical Sciences*. Roč. 113, s. 77-94. Available at: `https://doi.org/10.1016/j.ejps.2017.09.003`.

[35] WATSON, John G.; TROPP, Richard J.; KOHL, Steven D.; WANG, Xiaoliang and CHOW, Judith C., 2017. Filter Processing and Gravimetric Analysis for Suspended Particulate Matter Samples. Online. *Aerosol Science and Engineering*. Roč. 1, č. 2, s. 93-105. Available at: `https://doi.org/10.1007/s41810-017-0010-4`.

[36] SONG, Yingshi; MAHER, Barbara A.; LI, Feng; WANG, Xiaoke; SUN, Xiao et al., 2015. Particulate matter deposited on leaf of five evergreen species in Beijing, China: Source identification and size distribution. Online. *Atmospheric Environment*. Roč. 105, s. 53-60. Available at: `https://doi.org/10.1016/j.atmosenv.2015.01.032`.

[37] LAIHO, Patrik; MUSTONEN, Kimmo; OHNO, Yutaka; MARUYAMA, Shigeo and KAUPPINEN, Esko I., 2017. Dry and Direct Deposition of Aerosol-Synthesized Single-Walled Carbon Nanotubes by Thermophoresis. Online. *ACS Applied Materials & Interfaces*. 2017-06-21, roč. 9, č. 24, s. 20738-20747. Available at: `https://doi.org/10.1021/acsami.7b03151`.

[38] HAIG, C.W.; MACKAY, W.G.; WALKER, J.T. and WILLIAMS, C., 2016. Bioaerosol sampling: sampling mechanisms, bioefficiency and field studies.

Online. *Journal of Hospital Infection*. Roč. 93, č. 3, s. 242-255. Available at: https://doi.org/10.1016/j.jhin.2016.03.017.

[39] GRIMM, Hans and EATOUGH, Delbert J, 2012. Aerosol Measurement: The Use of Optical Light Scattering for the Determination of Particulate Size Distribution, and Particulate Mass, Including the Semi-Volatile Fraction. Online. *Journal of the Air & Waste Management Association*. 2012-01-24, roč. 59, č. 1, s. 101-107. Available at: https://doi.org/10.3155/1047-3289.59.1.101.

[40] MEDISANA. *Medisana Inhalator IN 500 Compact manual*. Online. MEDISANA. Medisana. Available at: https://www.medisana.com/en/Docs/?artnum=54520.

[41] LIBBLE. *Dittmann IHG 375 - Inhaler Manual*. Online. Libble. Available at: https://www.libble.eu/dittmann-ihg-375---inhaler/online-manual-799963/.

[42] OMRON. *Omron U100 microair nebulizer*. Online. OMRON. Omron. Available at: https://omronhealthcare.com/products/portable-microair-nebulizer-neu100/.

[43] COPLEY SCIENTIFIC. *Alberta Idealised Throat (AIT)*. Online. COPLEY. Copley Scientific. Available at: https://www.copleyscientific.com/inhaler-testing/realistic-throat-and-nasal-models/alberta-idealised-throat-ait/.

[44] PASTEKA, Richard; FORJAN, Mathias; SAUERMANN, Stefan and DRAUSCHKE, Andreas, 2019. Electro-mechanical Lung Simulator Using Polymer and Organic Human Lung Equivalents for Realistic Breathing Simulation. Online. *Scientific Reports*. Roč. 9, č. 1. Available at: https://doi.org/10.1038/s41598-019-56176-6.

[45] QOSINA. *One Way Valve*. Online. Available at: https://www.qosina.com/one-way-valve-97352.

[46] SENSIRION. *Proximal flow sensor for respiratory devices*. Online. Available at: https://www.sensirion.com/products/catalog/SFM3300-D/.

[47] JUDGE, Eoin P.; HUGHES, J. M. Lynne; EGAN, Jim J.; MAGUIRE, Michael; MOLLOY, Emer L. et al., 2014. Anatomy and Bronchoscopy of the Porcine Lung. A Model for Translational Respiratory Medicine. Online. *American Journal of Respiratory Cell and Molecular Biology*. Roč. 51, č. 3, s. 334-343. Available at: https://doi.org/10.1165/rcmb.2013-0453TR.

[48] PALAS. *Palas Promo 2000 Operation Manual*. Online. ManualsLib. Available at: https://www.manualslib.com/manual/2085485/Palas-Promo-2000.html#manual.

[49] PASTEKA, Richard; SCHÖLLBAUER, Lara Alina; SANTOS DA COSTA, Joao Pedro; KOLAR, Radim and FORJAN, Mathias, 2022. Experimental Evaluation of Dry Powder Inhalers during Inhalation and Exhalation Using a Model of the Human Respiratory System (xPULM). Online. *Pharmaceutics*. Roč. 14, č. 3. Available at: https://doi.org/10.3390/pharmaceutics14030500.

[50] PENNER, Thomas; BERGER, Simon; NIESSNER, Jennifer and DITTLER, Achim, 2022. Generation, characterization, and comparison of human exhaled and technical aerosols for the evaluation of different air-purifying technologies against infectious aerosols. Online. *Journal of Occupational and Environmental Hygiene*. 2022-11-02, roč. 19, č. 10-11, s. 646-662. Available at: https://doi.org/10.1080/15459624.2022.2125520.

[51] MITCHELL, Jolyon P. and SUGGETT, Jason A., 2014. Developing Ways to Evaluate in the Laboratory How Inhalation Devices Will Be Used by Patients and Care-Givers: The Need for Clinically Appropriate Testing. Online. *AAPS PharmSciTech*. Roč. 15, č. 5, s. 1275-1291. Available at: https://doi.org/10.1208/s12249-014-0145-4.

[52] MICHIGEN INSTRUMENTALS. *Training Test Lung - Test Lung Operation Manual*. Online. Available at: https://www.michiganinstruments.com/wp-content/uploads/2021/01/TTL3OpsManualREV2021-01.pdf.

[53] MICHIGEN INSTRUMENTALS. *Adult/Infant Lung Training and Testing*. Online. Available at: https://www.michiganinstruments.com/wp-content/uploads/2018/11/1601manual3.pdf.

List of Figures

List of Tables

Symbols and abbreviations

COPD	Chronic Obstructive Pulmonary disease
CFTR	Cystic Fibrosis Transmembrane Conductance Regulator
pMDIs	Pressurized Metered-Dosed Inhalers
DPIs	Dry Powder Inhalers
SMIs	Soft Mist Inhalers
MMAD	Mass Median Aerodynamic Diameter
CPC	Condensation Particle Counter
PET	Positron Emission Tomography
AUAM	Alberta Upper-Airway Model
PLA	Polylactic Acid
xPULM	Electromechanical breathing simulator
CPAP	Continuous Positive Airway Pressure
PN	Particle Number
PNC	Particle Number Concentration
MPD	Mean Particle Diameter
PM	Particulate Matter

List of appendices

A Protocol 1 - Nebulizer characterization

The first protocol captures the working procedure of characterization measurement of nebulizer devices, whose purpose is to evaluate the performance of each nebulizer device.

1. Filling the nebulizers chamber with physiological solution with the volume predefined by their manufacturer.
2. Pre-measurement weighting of the nebulizer device.
3. Turning on the breathing simulator and stabilizing for 30 seconds.
4. Turning on the spectrometer's pump and stabilizing for 30 seconds.
5. Connecting the nebulizer device to the measurement setup.
6. Turning on the nebulizer device, nebulizing for 3 minutes.
7. Turning off the nebulizer device.
8. Post-measurement weighting of the nebulizer device.
9. Repeating the measurement for 3 times in a row.
10. Turning off the breathing simulator.
11. Post-measurement calculations: Obtaining particle numbers and number concentrations, particulate matter values, and particle diameters from optical spectrometers. Computing the aerosol output, aerosol output rate, mean particle diameter, residual volume, and percentage of emitted volume per minute.

B Protocol 2 - Aerosol particle deposition measurement

The second protocol captures the working procedure of respiratory measurement of nebulizer devices, whose purpose is to evaluate the changes in the particle diameter and in the particle number concentration when passing through respiraory tract represantation and the total deposition fraction.

1. Filling the nebulizers chamber with physiological solution with the volume predefined by their manufacturer.
2. Turning on the breathing simulator and stabilizing for 30 seconds.
3. Turning on the spectrometer's pump and stabilizing for 30 seconds.
4. Connecting the nebulizer device to the measurement setup.
5. Turning on the nebulizer device, nebulizing for 1 minute.
6. Turning off the nebulizer device.
7. Turning off the breathing simulator.
8. Post-measurement calculations: Obtaining the values of particle diameter, particulate matter, and particle numbers and number concentrations measured throughout the whole measurement. Analyzing the changes in particle size distributions, particle diameters, and particulate matter. Computing the total deposition fraction.